NBER WORKING PAPER SERIES

AGGREGATE LAPSATION RISK

Ralph S. J. Koijen
Hae Kang Lee
Stijn Van Nieuwerburgh

Working Paper 30187
http://www.nber.org/papers/w30187

NATIONAL BUREAU OF ECONOMIC RESEARCH
1050 Massachusetts Avenue
Cambridge, MA 02138
June 2022

We gratefully acknowledge the data support from the Life Insurance Company. Koijen acknowledges financial support from the Center for Research in Security Prices at the University of Chicago and the Fama Research Fund at the University of Chicago Booth School of Business. For comments and suggestions, we thank Michael Gallary, Sears Merritt, and seminar participants at Rutgers business school. The views expressed herein are those of the authors and do not necessarily reflect the views of the National Bureau of Economic Research.

Aggregate Lapsation Risk
Ralph S. J. Koijen, Hae Kang Lee, and Stijn Van Nieuwerburgh
NBER Working Paper No. 30187
June 2022
JEL No. E32,E44,G12,G22,G52

ABSTRACT

We study aggregate lapsation risk in the life insurance sector. Using the regulatory reporting of historical lapse rates by life insurers, we empirically document the counter-cyclicality of lapsation behavior. We construct two lapsation risk factors that explain a large fraction of the common variation in lapse rates of the 30 largest life insurance companies. The first is a cyclical factor that correlates with credit spreads and employment, while the second factor is a trend factor that correlates with the level of interest rates. Using a novel policy-level database from a large life insurer, we examine the heterogeneity in risk factor exposures based on policy and policyholder characteristics. Young policyholders with higher health risk are more likely to lapse their policies during economic downturns. We explore the implications for hedging and valuation of life insurance contracts. Ignoring aggregate lapsation risk results in cross-subsidization across policyholders with different lapsation risk, and in a mispricing of life insurance policies. Our results have implications for the welfare costs of business cycles.

Ralph S. J. Koijen
University of Chicago
Booth School of Business
5807 S Woodlawn Ave
Chicago, IL 60637
and NBER
Ralph.koijen@chicagobooth.edu

Stijn Van Nieuwerburgh
Columbia University
Graduate school of Business
Uris Hall, office 809
3022 Broadway
New York, NY 10027
and NBER
svnieuwe@gsb.columbia.edu

Hae Kang Lee
University of South Carolina
Darla Moore School of Business,
Room 427A
haekang.lee@moore.sc.edu

1 Introduction

Life insurance is a key risk management tool for households when it comes to managing the tail risk associated with the premature death of a family member. One understudied fact about life insurance policies is that households lapse them frequently. To the extent that this phenomenon has been studied, the literature has primarily focused on idiosyncratic lapsation risk. We document that there is a large common component in lapsation that varies systematically over the business cycle. Furthermore, life insurance contracts with different policy and policyholder characteristics are differentially exposed to these common lapsation factors. When young or low-income households lapse their policies in a recession, that has long-lasting consequences for their economic well-being, contributing to the cost of business cycles. These new facts not only have implications for households but also for life insurers, since the systemic variation in lapsation rates affects the valuation and risk mismatch on the balance sheets of insurance companies.

To start, we use regulatory data from the 30 largest life insurance companies from 1996 to 2020 to measure the dynamics and co-movement of lapsation rates. We decompose the lapsation rate of each company into a trend and a cycle component. We then extract the first principal component of the trend components and the first principal component of the cycle components. The first principal components explain the bulk of the variation across years and companies. The first factor, which we label the trend factor, captures a secular decline in lapsation rates, from a little over 7% per year in the beginning of our sample to approximately 5% at the end of our sample. The dynamics of this factor follows the trend in the level of interest rates. The second factor captures the counter-cyclicality in lapsation rates. This cycle factor correlates strongly with credit spreads and macroeconomic conditions. We illustrate the co-movement between the cycle factor and employment (left panel) and GDP (right panel) in Figure 1.

With the aggregate lapsation factors in hand, we explore how exposure to these factors varies with policy and policyholder characteristics. We exploit a new proprietary data set from a large US life insurance company for this part of the analysis. We have detailed data on the terms of the life insurance policy (including term or whole life insurance, the length of the term, and the size of the policy) and policyholder characteristics (including age, health status, zip code, and gender).

We find that young policyholders are more exposed to the cycle factor. As these policyholders are likely to be first-time life insurance buyers, there could be important long-term effects if lapsation lowers the likelihood that these policyholders buy life insurance in the future. Second, we find that policyholders with higher health risks are more likely to lapse their policies during economic downturns.

Figure 1. **Lapse Cycle and Macro Variables**

This figure plots the lapse cycle factor against macroeconomic variables. The red dotted line in both panels represent the lapse cycle factor. The black line in the left panel represents the cyclical component of employment ("Filtered Employment"). The black line in the right panel represents the cyclical component of GDP ("Filtered GDP").

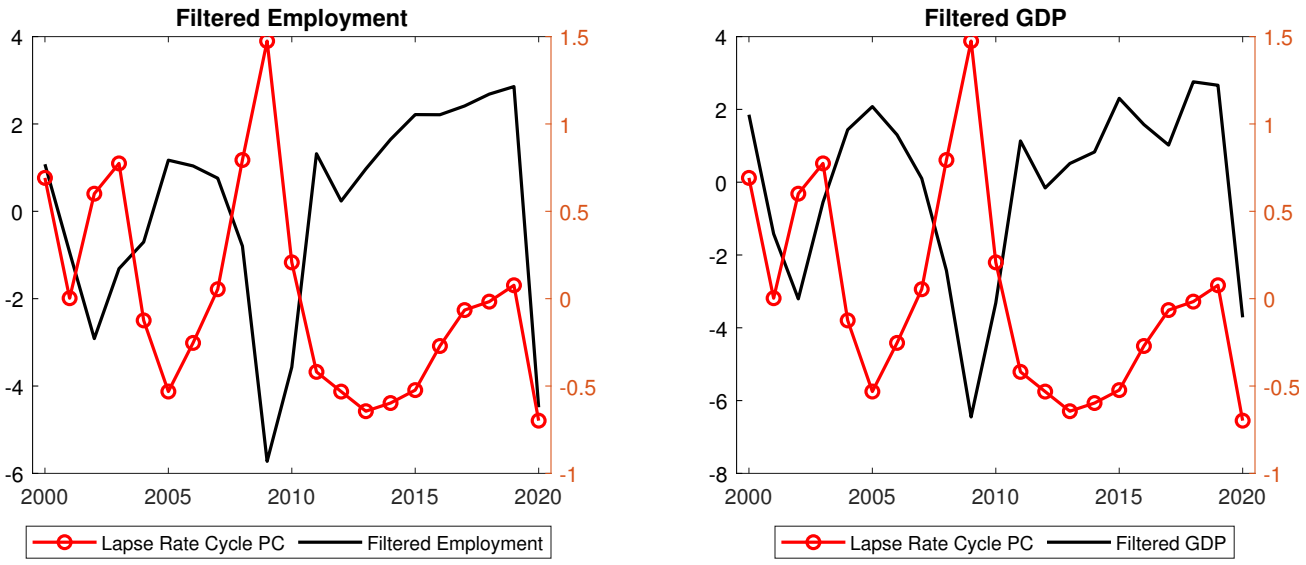

These findings are not only relevant to households, and to understanding the cross-subsidization across groups of households, but also to life insurance companies. In particular, as a result of the correlation between lapsation and aggregate economic conditions, the valuation of life insurance policies is affected. Since lapsation is high during economic downturns, when investors' marginal utility is high, the effective lapsation rate is higher when accounting for aggregate risk. Formally, the risk-neutral lapsation rate is higher than the physical lapsation rate.

We explore how lapsation rates are reflected in life insurance valuations. There are two opposing forces. On the one hand, when insurance companies underwrite policies, they pay a commission to the insurance broker. If the policy is more likely to lapse early, the insurer may not yet have recovered the broker's commission, and ignoring aggregate lapsation risk would lead to a premium that is too low. We refer to this as the "fixed-cost effect." On the other hand, a key feature of life insurance contracts is that the premium paid is flat over the life of the contract. Since mortality risk increases with age, insurers profit during the first years of the contract (when the cost of mortality cover is below the premium) and lose money during the later years of the contract (when the cost of mortality cover exceeds the premium). If insurers ignore aggregate lapsation risk, and use a lapsation rate that is too low, they put too much weight on the later years of the contract that are unprofitable. The

insurance premium charged would therefore be too high. We refer to his as the "mortality effect."

Given these opposing forces, it is a quantitative question how aggregate lapsation risk affects life insurance valuation. We develop an asset pricing model that captures the observed correlation of lapsation rates with financial market variables. The model is calibrated to match the prices of Treasury and corporate bonds. We find that the mortality effect outweighs the fixed-cost effect. In our calibration, profits on a 20-year life insurance contract sold to a healthy 40-year old are about 30% higher than they would be if the contract was correctly priced. Premiums are about 3% too high. We also find that the excess profits are higher in a low interest rate environment.

The Covid-19 pandemic, which occurs at the end of our sample, presents an interesting perspective. Unlike in the two previous recessions, the lapsation rate falls in 2020. We conjecture that, first, the coronavirus increased the salience of mortality risk, and brought renewed urgency to not letting insurance policies lapse and, second, that the government's unusually generous transfer spending (stimulus checks, extended unemployment insurance) enabled households to continue paying their insurance premiums in the face of economic hardship.

Related Literature There is a strand of the insurance literature studying the lapsation in the life insurance sector. These studies mainly focus on the demand side of lapsation, for example which policyholders characteristics explain the observed lapse patterns. Society of Actuaries and LIMRA (2019) is the standard industry source aggregating the lapse experience data of member firms. Eling and Kiesenbauer (2013) use policyholder-level data from Germany to investigate which policy and policyholder characteristics drive the lapse patterns in the data. Milliman (2020) document similar lapse patterns, focusing on the post-term period where the premium spikes.

Hendel and Lizzeri (2003) theoretically and empirically show how the front-loading of insurance policies affects lapse behavior by comparing renewable term policies to level-payment term policies.

Gottlieb and Smetters (2021) provide behavioral explanations for the high observed lapse rates. They conduct a survey to document that policyholders systematically underestimate their own lapse probabilities at the time of policy purchase. A separate survey for those who have just lapsed reports that the two main sources of lapsation are forgetfulness and liquidity needs. Our paper complements their analysis by focusing on aggregate risk.

Kuo, Tsai, and Chen (2003) use annual aggregate lapse rates between 1951 to 1998 to analyze econometric relationships of lapse rates with interest rates and unemployment rates. We focus on the period after 1998 to document the cyclicality of lapsation. We also use novel data to document differential exposures of insurers and policyholders to the aggregate risk

factors. Lastly, by using calibrated asset pricing model, we study the pricing implications of aggregate lapsation risk.

Our paper is also related to a large literature on prepayment risk in mortgage contracts. See for instance Schwartz and Torous (1989), Stanton (1995), Deng, Quigley, and Order (2000), Boyarchenko, Fuster, and Lucca (2019), Chernov, Dunn, and Longstaff (2018), and Diep, Eisfeldt, and Richardson (2021). In this literature, it is well understood that modeling prepayment risk and the covariance of prepayment rates with priced aggregate risk factors is essential to determine the correct valuation of a mortgage or a pool of mortgages (mortgage-backed security). Real-world mortgage prepayment behavior responds to interest rates (the rate incentive) and variables that move with the business cycle like employment or house prices. But it also contains behavioral aspects that are harder to capture with a rational model. In another parallel, the recent mortgage literature has emphasized that suboptimal prepayment behavior can lead to cross-subsidization and redistribution (Gerardi, Willen, and Zhang (2021), Zhang (2022) and Fisher et al. (2021)). We show that lapsation rates are also exposed to priced aggregate risks, that accounting for these aggregate risks is important in computing insurance premiums, and that cross-sectional differences in actual lapsation behavior has distributional consequences when it is not reflected in insurance premiums.

2 Data

2.1 S&P Global Market Intelligence

To study aggregate lapsation risk, we analyze two databases. The first database is S&P Global Market Intelligence (SNL), which contains the universe of regulatory filings by insurance companies. We focus on life insurance companies and exclude property and casualty insurance companies. The data are at the annual frequency, spanning 1996 to 2020 (the lapse rate starts in 1997). SNL offers data at two different levels of granularity: at the company level (company codes starting with "C") or at the group level (company codes starting with "GK"). We use group-level data in our baseline analysis. For robustness, we also repeat the same analysis using corporate-level data, and find that the analysis does not meaningfully change. We refer to *firm* or *firm-year* to represent the entities in the group-level data (that is, "GK" companies).

The main variable of interest is the lapse rate observed at a yearly frequency. We use the term "lapsation rate" to include both the lapsation and surrender, following the standard definition used in the industry (Society of Actuaries and LIMRA, 2019). We use the lapsation rate for ordinary life insurance (that is, individual life insurance), retrieved from the

Ordinary Life: Lapse & Surrender Ratio time series of the SNL dataset.[1] We drop the following five insurance groups: SCOR U.S. Only (GK4020905), RGA U.S. Only (GK103450), Swiss Re U.S. Only (GK4290308), Hannover Life Reassurance (C2749), and Munich Re U.S. Only (GK4005715). These companies are either international or reinsurance companies. For the regression analysis, we drop outliers with lapsation rates greater than 30%, which removes 2.8% of the lapsation rate observations.

2.2 Macro Variables

We construct two macro variables, GDP and Employment, at the firm-year level. Specifically, we start from state-level macro time series data from the FRED database of the St. Louis Fed. For GDP, we use the annual *Real Total Gross Domestic Product* series for each state. The time series starts in 1997. We extend this series back to 1993 by regressing GDP growth rates of each state on state-level employment growth rates and the aggregate GDP growth rate.

We then apply the Hamilton (2018) filter to the annual series of the state-level log GDP to obtain its cyclical component. For Employment, we use the seasonally-adjusted monthly *All Employees: Total Nonfarm* time series for each state. We apply the Hamilton filter to the log level of employment, and take the annual average of the filtered values. For each firm-year, we use the share of total life insurance premium income (*Life ex Annuity: Sate Direct Premiums & Annuity Considerations (in $000)* from S&P Global Market Intelligence) in each U.S. state as the weight vector to calculate firm-specific macro variables. This process generates our firm-year level macro time series.

Aggregate macro variables are also retrieved from the FRED database of the St. Louis Fed. For GDP, we use the annual *Real Gross Domestic Product* series (GDPCA). We apply the Hamilton filter to the annual series of the log GDP. For employment, we first retrieve the monthly *All Employees, Total Nonfarm* series (PAYEMS), and apply the Hamilton filter to the monthly series to decompose the trend and the cycle.[2] We then take the annual average of the monthly cycle to construct an annual employment cycle series.

For interest rates, we use the *10-Year Treasury Constant Maturity Rate* (GS10), where we convert the monthly rates into annual rates by taking averages. For credit spreads, we use

[1] Data is accessed on April 18, 2021. Note that S&P Global Market Intelligence retrospectively updates historical financial data to reflect the latest corporate structures following M&As and other corporate activities. In "Group Methodology Summary on MI" document, it states *"Market Intelligence Groups are composed of members within that corporate structure on an as-is basis. Structures are updated quarterly and amended for any mergers or acquisitions. The current members' composition is applied retrospectively to all financial data for all periods."*

[2] The Hamilton filter described in Hamilton (2018) can be applied to both annual and monthly time series with different choices of (h, p) for the regression $y_{t+h} = d_0 + \sum_{j=1}^{p} d_j y_{t-j+1} + c_{t+h}$. We use the recommended parameter value of $h = 2$ for annual series and $h = 24$ for monthly series. We also use $p = 2$ for annual series and $p = 12$ for monthly series, which look back one year for the lagged regressors, consistently with the recommended choice of $p = 4$ for quarterly series.

Moody's Seasoned Baa Corporate Bond Yield Relative to Yield on 10-Year Treasury Constant Maturity (BAA10YM) and follow similar procedure to obtain an annual time series. We average these series as lapsation occurs during the year.

For the county-level analysis, we use the median house price from Zillow. Specifically, we take the average of the monthly ZHVI index over each year to construct the annual series. The county-level unemployment rate data is downloaded from the BLS Local Area Unemployment Statistics (LAUS).

2.3 Policy-level Insurance Database

The second and main novel proprietary database is provided to us by a major *Life Insurance Company*. This is a large database of life insurance contracts, containing policy-level details. The database is de-identified by a third party vendor for research purposes, so that we cannot recover the identity of policyholders. We observe policy characteristics, such as size, policy type (whole life, term life, or other), policy status (in-force, lapsed, or surrendered) and issuance date. We also observe detailed policyholder characteristics such as age, gender, smoking status, risk class, and ZIP code. Hereafter, we will refer to this database as the Firm Database for convenience. The database contains life insurance policies spanning from late 1998 to early 2016.

As part of our data validation process, we compare the lapse rates of the Firm in the S&P database (see Section 2.1) with the aggregate lapse rates we construct using the Firm Database. If the Firm Database is representative of the firm's portfolio of insurance policies, the two lapsation rates should be close. We present a comparison in Figure 2. The orange line plots the lapsation rate from the S&P database, while the blue line plots the aggregate lapse rate calculated from the Firm Database. In the early period from 1999–2004, there is a wide discrepancy between the two lines. This discrepancy is due to the left-truncation of the Firm Database, which only contains new policies originated after late-1998. To see this, note that the lapse rate in year t is calculated using the following equation:

$$LapseRate_t = \frac{\text{Policies Lapsed within Year } t}{0.5\,(\text{In-Force Beginning of Year } t + \text{In-Force End of Year } t)} \tag{1}$$

where the numerator and the denominator can be based on either the number of policies or the amount of face value.

Since we only observe the policies issued by the *Insurance Company* on or after 1998, it takes a few years until the in-force policy pool populates and the denominator stabilizes. Similarly, at the end of the sample, the two lines diverge as we do not observe policies in the firm-level database that were originated after 2016. In between these two periods, our

firm-level data set tracks the aggregate lapse rate well.

Figure 2. **Aggregate Lapse Rate Validation**

This figure presents the validation exercise we perform to ensure the coverage of the Firm Database we use. The blue line plots the aggregate lapse rate we directly calculate from the Firm Database using Equation (1). The orange line plots the reported aggregate lapse rate from the S&P Global Market Intelligence database. Two graphs are reasonably close after 2003, which validates our use of the database. There is some discrepancy early in the period due to left truncation of the database, see Section 2.1 for details.

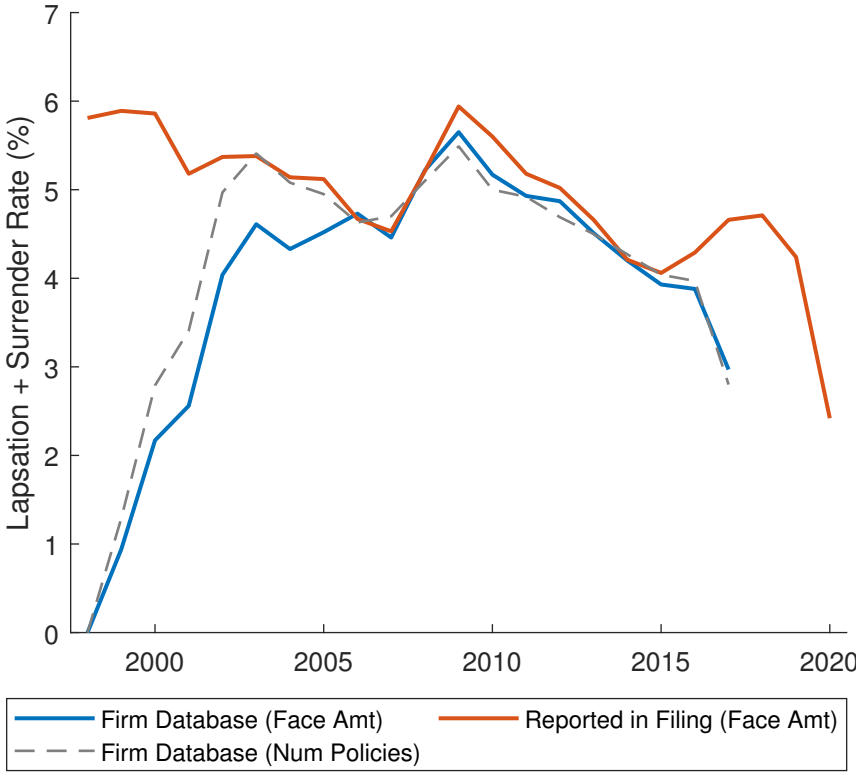

3 Empirical Methodology

3.1 Principal Component Analysis

For each of the 30 largest[3] life insurance companies, as defined by in-force policy amount outstanding as of 2020, we start from the historical lapsation rate series from 1997 to 2020

[3]We skip the 30th largest life insurance company, Resolution Life Holdings Inc (GK26554449), because it has the 2010 lapsation rate missing. Instead we include the next largest company, Penn Mutual (GK110258). The PCA results do not fundamentally change when we use the Resolution Life Holdings Inc with the overridden lapsation rate 0.80% for 2010, which is the best estimate based on the *Insurance In Force*, *Insurance Lost: Lapsed* and *Insurance Lost: Surrendered* variables.

and apply the Hamilton filter to decompose the lapse rate time series into a trend and cycle component. We then separately run two principal component analyses, one using the trend time series and one using the cycle time series. Starting from the 30 trend time series, we construct the first principal component that explains most of the variation using the correlation matrix, and denote it as the *Lapse Trend factor*. Similarly, we define the *Lapse Cycle factor* as the first principal component of the 30 cycle time series. We use the *Lapse Trend factor* and the *Lapse Cycle factor* as the aggregate lapsation risk factors.

3.2 Firm-level Lapsation Analysis

We first study the heterogeneity in aggregate lapsation risk exposure at the firm-level. The firm-level time series of lapsation rates can be used to run the following factor regression with the lapsation risk factors constructed in 3.1:

$$Lapse\,Rate_t^j = \alpha^j + \beta^j_{Trend} Lapse\,Trend_t + \beta^j_{Cycle} Lapse\,Cycle_t + \varepsilon^j_t, \tag{2}$$

where j represents the index for firm j.

3.3 Policy-level Lapsation Analysis

Next, we investigate the heterogeneity in exposures to aggregate lapse risk factors by policy and policyholder characteristics, utilizing the micro-level Firm Database. To this end, we estimate a Cox proportional hazard model of the observed lapse events on the time-varying characteristics. For policy j issued at time t, we specify the annual lapsation hazard rate at time $t + \tau$ as:

$$\lambda_{j,t+\tau} = \lambda_0(\tau) \exp(\boldsymbol{\beta' Z_{j,t+\tau}}) \tag{3}$$

where $\lambda_0(\tau)$ is the baseline hazard rate at policy age $\tau \geq 1$, and the log relative risk is linear in the vector of characteristics $Z_{j,t+\tau}$. Most of the policy or policyholder characteristics (for instance, gender, smoking status, risk class, and term life policy indicator) are time-invariant. For each policy or policyholder characteristic z^i_j (or $z^i_{j,t+\tau}$ if time-varying characteristic), we additionally include the interaction term with the lapse cycle factor, i.e. $z^{i,cycle}_{j,t+\tau} = z^i_j \times (Lapse\,Cycle)_{t+\tau}$ in the characteristic vector $\boldsymbol{Z_{j,t+\tau}}$. The estimated coefficients on these interacted variables allow us to understand how the exposure to the cycle factor varies with policy and policyholder characteristics.[4]

[4]We can similarly include the interaction terms with the lapse trend factor. Our main interest is the heterogeneous exposure on the lapse cycle risk factor, so we do not include the lapse trend interactions in the

3.4 Geographical Analysis

We investigate the geographical variation in lapse rate changes between 2006 and 2009 at the county-level. As the severity of the economic downturn varies across geographies, it provides us another way to explore how economic conditions relate to lapse rates. Specifically, we study the relationship with county-level economic variables such as house price changes and unemployment rate changes. The Firm Database contains the policyholders' ZIP codes for about 95% of our sample, so we first map the ZIP code information to the corresponding county's FIPS code by using the HUD USPS ZIP code-to-county crosswalk.[5] There are 3,049 counties in the database, and the Firm's life insurance business is concentrated in larger and more populous counties. As the lapsation calculation becomes noisy for counties with little coverage, we drop counties with fewer than 100 policies issued in our sample. This leaves us with 826 counties, representing 96% of life insurance face amount coverage of the overall sample. Data on changes in house prices from Zillow (ZHVI) are available for 762 counties (92%), changes in unemployment rates are available for 823 counties (99.6%), and both variables are available for 759 counties (92%). Our results are not sensitive to reasonable variations in the 100 policy threshold.

We construct three county-level variables to measure the change in lapsation rates, housing prices, and the unemployment rates between 2006 and 2009,

$$
\begin{aligned}
(\Delta Lapse\, 06-09)_c &= (Lapse_{c,2009} - Lapse_{c,2006}) \times 100, \\
(\Delta HousingPrice\, 06-09)_c &= \left(\frac{ZHVI_{c,2009}}{ZHVI_{c,2006}} - 1\right) \times 100, \\
(\Delta Unemp\, 06-09)_c &= (Unemp_{c,2009} - Unemp_{c,2006}) \times 100.
\end{aligned}
$$

We then regress $(\Delta Lapse\, 06-09)_c$ on the house price change and the unemployment rate change. The baseline specification is least squares, where observations are weighted by the average in-force amount in 2006. This variable is the denominator used in the lapse rate calculation formula. Intuitively, it represents the size of insurance business in each county as of 2006.

baseline specification. Including the interaction terms with the lapse trend factor does not materially change the coefficients on the interacted variables with the lapse cycle factor.

[5] https://www.huduser.gov/portal/datasets/usps_crosswalk.html. We use the union of 2010, 2013, 2016 and 2019 Q1 versions, where the latest mappings were used per ZIP code.

4 Empirical Results

4.1 Factor Construction

Following the empirical procedure described in Section 3.1, we construct two lapsation risk factors from the 30 lapse trend components and the 30 lapse cyclical components. These 30 largest firms in the SNL database represent about the 81.2% of the market based on the in-force policy size at the end of 2020.

Figure 3 plots the aggregate lapsation risk factors. The *Lapse Trend factor*, which is the first principal component of the lapse trend time series, explains 96.4% of variation in firms' lapse trends. The *Lapse Cycle factor* similarly explains 69.5% of variation in firms' lapse cycles. These two factors explain a large part of the common variation in lapsation rates across firms, and we use these factors as the aggregate lapse risk factors.

One salient fact is the gradual decline in the *Lapse Trend factor*. Coinciding with the secular decline in interest rates, lapse rates have also been declining over the past 20 years as depicted for several large firms in Figure 4. The *Lapse Trend factor* captures this industry-wide decline. The co-movement with interest rates is illustrated in the upper panel of Figure 5.

Table 1 formalizes this relationship by regressing the *Lapse Trend factor* on the 10-year Treasury rate and other business cycle variables such as aggregate Filtered GDP, aggregate Filtered Employment, and the Baa credit spread over the 10-year Treasury rate. The positive and statistically significant coefficients on the 10-year Treasury rate, along with insignificant coefficients on the business cycle variables indicate that the *Lapse Trend factor* primarily moves with interest rates. Lower rates increase the present value of the death benefit, and hence the value of a life insurance contract, making it more costly to lapse from the policyholder's perspective. Lower rates also increase the cost (premium payments) of a new policy, again increasing the cost of lapsing an existing contract that was signed when rates were higher. We do caution that identifying relationships between trending variables is challenging, and we therefore interpret this evidence as suggestive of a link between the trends in lapsation rates and interest rates.

The *Lapse Cycle factor* on the other hand mostly captures the business cycle effect. Figure 1 plots the *Lapse Cycle factor* against two filtered macro variables, employment and GDP. The counter-cyclicality of the *Lapse Cycle factor* is clear from the graphs.[6] The lower panel of Figure 5 shows that the factor is positively correlated with the Baa credit spread, a financial market variable known to be closely related to the business cycle.

Table 2 formalizes this relationship by estimating similar models as in Table 1. Two obser-

[6]The principal component analysis is agnostic on the sign of the factor. We construct the factor to be countercyclical instead of being procyclical.

Figure 3. **The Evolution of Lapse Trend and Lapse Cycle**

This figure plots the aggregate lapsation factors we construct. For each company, we start from the historical lapse rate series from 1997 to 2020, and apply Hamilton filter to decompose the lapse rate time series into the trend time series and the cycle time series. We then separately run two principal component analyses to the trend time series and the cycle time series. Starting from the 30 trend time series, we construct the first principal component that explains the most of the variations using the correlation matrix, and denote it as the *Lapse Trend factor*. Similarly, we define the *Lapse Cycle factor* as the first principal component of the 30 cycle time series.

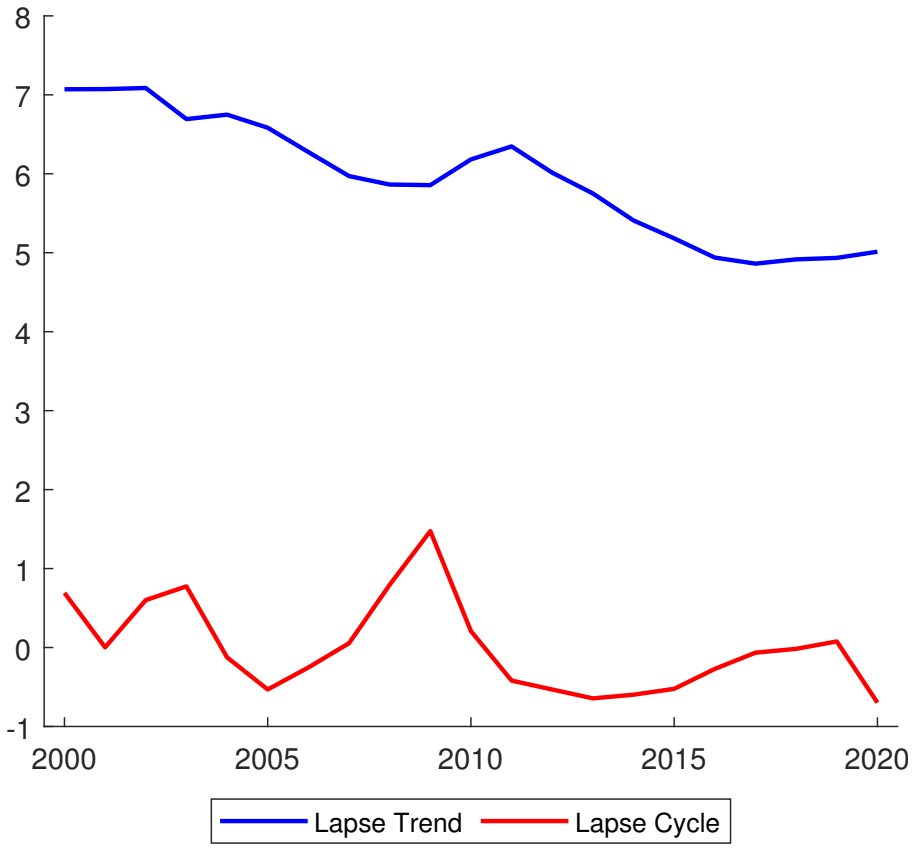

Figure 4. **Lapse Rates vs. Macro Variable (GDP) of the Largest Life Insurers**

This figure plots the historical lapse rates against the firm-specific filtered GDP of the 12 largest insurance groups from the S&P Global Market Intelligence Database. For each life insurance company, the company-relevant GDP is calculated as the weighted-average of the state-level GDP, where the weights are based on the gross premium income from each state to reflect the economic exposures to each state.

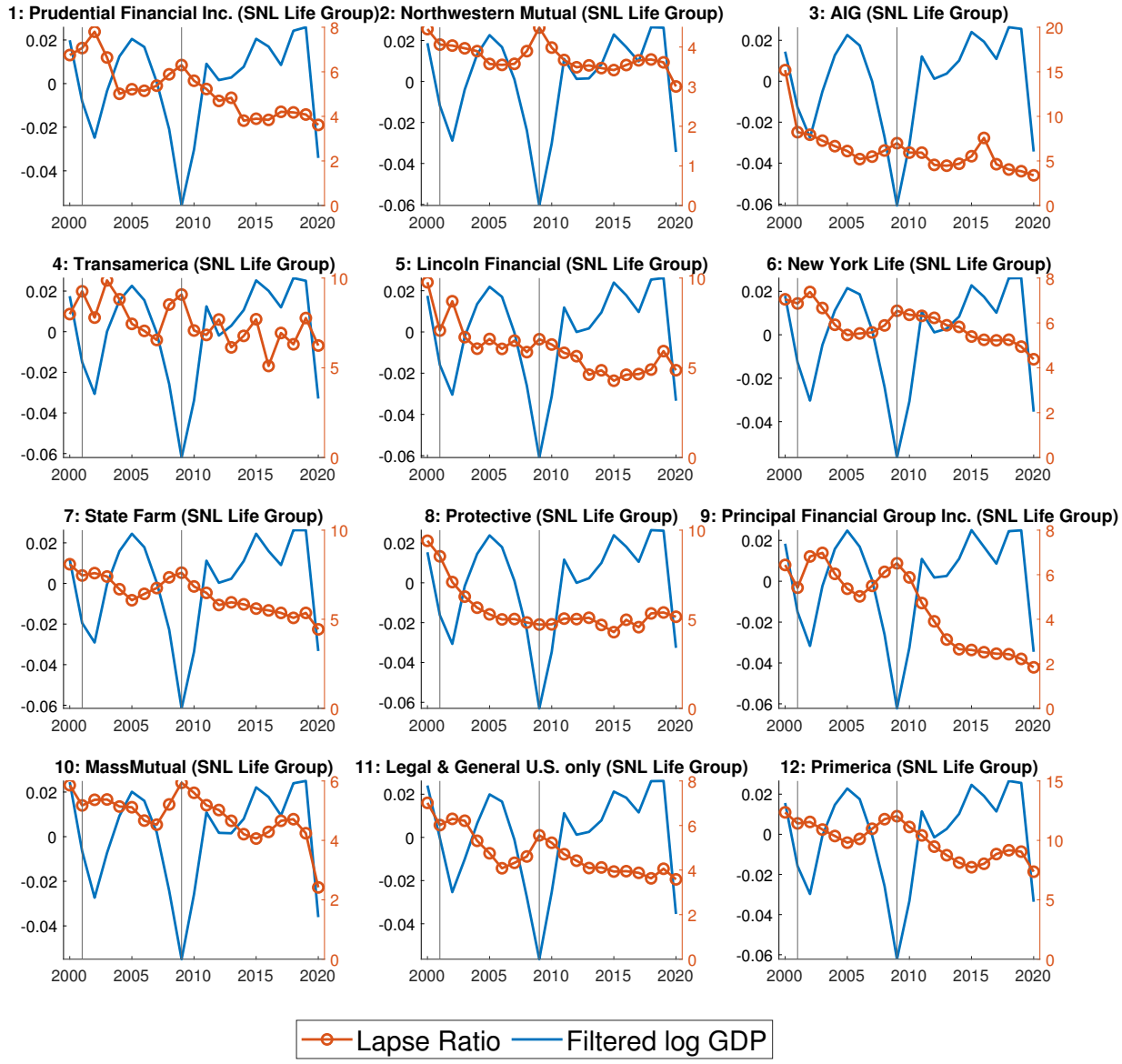

Table 1. **Time Series Regression of Lapse Trend**

This table presents the results of the following time-series regressions:

$$Lapse\ Trend\ Factor_t = \beta\,(\text{Treasury 10y})_t + \gamma X_t + \varepsilon_t$$

for year t, where the business cycle variable X_t indicates either the Filtered GDP, Filtered Employment, or Baa Credit spread over 10y. Robust standard errors are reported in parentheses.

	(1)	(2)	(3)	(4)	(5)
Treasury 10y	0.478***	0.479***	0.465***	0.506***	0.470***
	(0.0688)	(0.0607)	(0.0578)	(0.0608)	(0.0544)
Filtered GDP		-0.0622			0.298***
		(0.0366)			(0.0769)
Filtered Employment			-0.0849**		-0.301***
			(0.0377)		(0.0520)
Baa Credit Spread over 10y				0.306	0.445**
				(0.185)	(0.180)
Constant	4.359***	4.351***	4.401***	3.463***	3.244***
	(0.266)	(0.239)	(0.233)	(0.565)	(0.455)
Observations	21	21	21	21	21
R^2	0.664	0.704	0.735	0.724	0.814
Adjusted R^2	0.646	0.671	0.706	0.693	0.768

Standard errors in parentheses

* p<0.1, ** p<0.05, *** p<0.01

Table 2. **Time Series Regression of Lapse Cycle**

This table presents the results of the following time-series regressions:

$$Lapse\,Cycle\,Factor_t = \beta\,(\text{Treasury 10y})_t + \gamma X_t + \varepsilon_t$$

for year t, where the business cycle variable X_t indicates either the Filtered GDP, Filtered Employment, or Baa Credit spread over 10y. Robust standard errors are reported in parentheses.

	(1)	(2)	(3)	(4)	(5)
Treasury 10y	0.210***	0.213**	0.195**	0.262***	0.255***
	(0.0549)	(0.0772)	(0.0807)	(0.0620)	(0.0694)
Filtered GDP		-0.124**			-0.113
		(0.0515)			(0.0976)
Filtered Employment			-0.106*		0.0597
			(0.0608)		(0.0859)
Baa Credit Spread over 10y				0.550***	0.366**
				(0.177)	(0.162)
Constant	-0.697***	-0.714**	-0.645**	-2.309***	-1.813***
	(0.186)	(0.279)	(0.300)	(0.581)	(0.548)
Observations	21	21	21	21	21
R^2	0.227	0.504	0.422	0.568	0.596
Adjusted R^2	0.186	0.449	0.358	0.520	0.495

Standard errors in parentheses

* p<0.1, ** p<0.05, *** p<0.01

vations are notable compared to the results in Table 1. First, the coefficients on the business cycle variables, Filtered GDP, and the Baa Credit Spread over the 10-year Treasury yield are all statistically significant at the 5% level, and the coefficient on Filtered Employment is statistically significant at the 10% level. The signs of the coefficients highlight the strong counter-cyclicality of the *Lapse Cycle factor*. Second, the coefficients on the 10-year Treasury yield are also statistically significant and positive. This indicates that the cyclical component of lapsation contains some exposure to declining interest rates.[7] Intuitively, the rise in the lapsation rate in recessions indicates that a subset of policyholders face economic hardship that no longer allows them to make premium payments.

[7]The *Lapse Trend factor* and the *Lapse Cycle factor* are *not* constructed as the first and the second principal component of a set of vectors, so there is no guarantee that these factors are uncorrelated. The constructed lapsation risk factors are positively correlated.

Table 3. **Hedging Opportunities using Financial Products**

This table presents the time-series regression results of the changes in lapsation risk factors on the change in 10-year Treasury rate and the change in Baa Credit Spread over 10-year Treasury yield. Robust standard errors are reported in parentheses.

	(1) ΔLapse Trend	(2) ΔLapse Cycle	(3) ΔLapse Total
ΔTreasury 10y	-0.103	0.551**	0.449**
	(0.124)	(0.224)	(0.158)
ΔBaa Credit Spread over 10y	-0.0897	0.693***	0.603***
	(0.117)	(0.188)	(0.0963)
Constant	-0.128***	0.0594	-0.0682
	(0.0432)	(0.0885)	(0.0875)
Observations	20	20	20
R^2	0.061	0.392	0.394
Adjusted R^2	-0.049	0.320	0.323

Standard errors in parentheses
* p<0.1, ** p<0.05, *** p<0.01

The top panel of Figure 5 plots the *Lapse Trend factor* against the 10-year Treasury yield. The bottom panel of Figure 5 plots the *Lapse Cycle factor* against the Baa credit spread over the 10-year Treasury yield. The strong comovement suggests that aggregate lapsation risk can be hedged with a portfolio of Treasuries and corporate bonds.

We formalize this intuition in Table 3 by regressing the change in lapse rates on the changes in financial market variables. Unlike in Table 1 and 2, we use changes in variables to establish the relationship, because the changes in variables are more relevant than the levels for hedging purposes. Column (1) suggests that the *Lapse Trend factor* is harder to hedge annually, and that there is a lower frequency relationship between the *Lapse Trend factor* and the 10-year Treasury Rate. Column (2) shows that the annual changes in *Lapse Cycle factor* can be effectively hedged using Baa-rated corporate bonds and Treasuries. In Column (3), we use the change in *Lapse Total* as a dependent variable, which is the sum of the *Lapse Trend factor* and the the *Lapse Cycle factor*. This final column shows that this simple hedging strategy already captures 40% of the variation in lapse rates.

4.2 Heterogeneity in Risk Factor Exposures

Equipped with the two aggregate lapsation risk factors, we investigate the heterogeneity in risk exposures across (i) life insurers by estimating the regression specified in Equation (2),

Figure 5. **Lapse Factors and Financial Market Variables**

This figure plots the lapsation factors against the financial market variables. The blue line in the upper panel plots the *Lapse Trend factor* against the 10-year Treasury yield. The red line in the lower panel plots the *Lapse Cycle factor* against the Baa credit spread over 10-year Treasury yield.

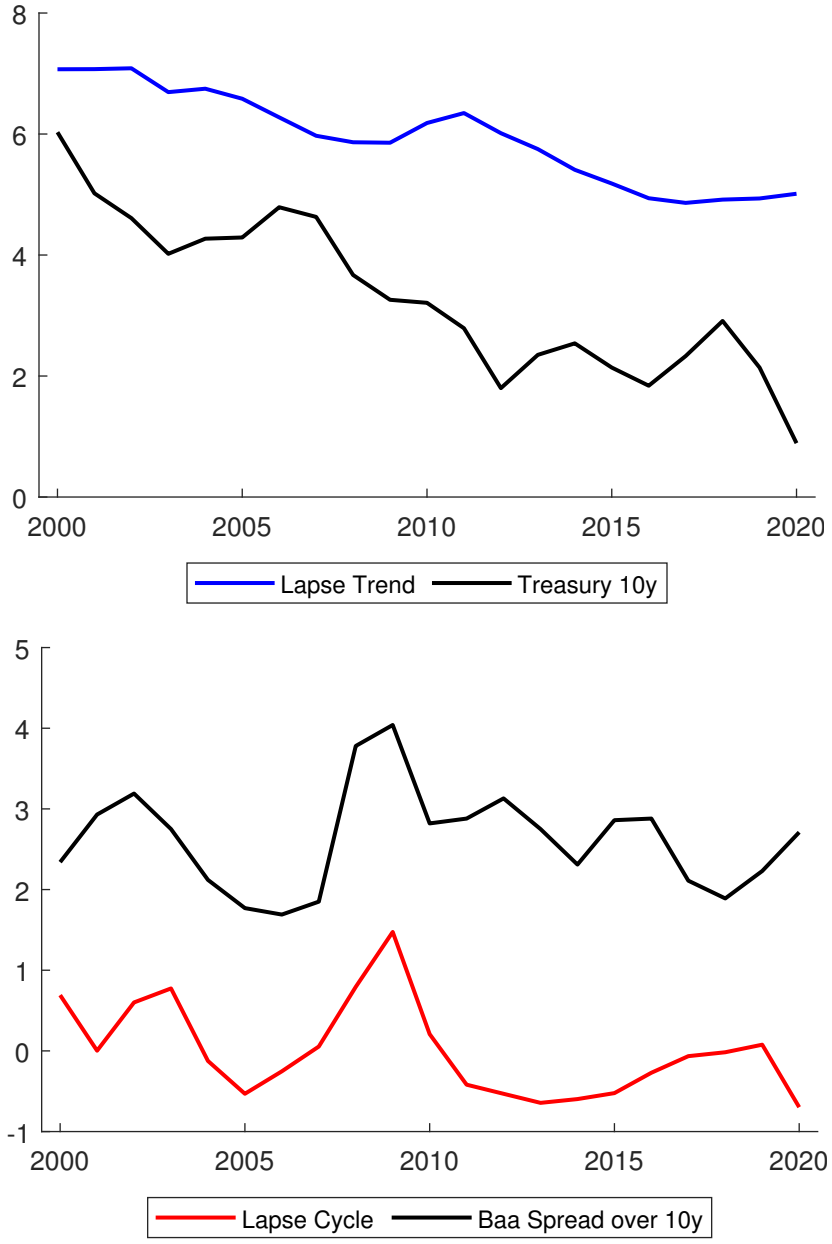

(ii) across individual policies by estimating the Cox proportional hazard model specified in Equation (3), and (iii) across geographies. First, we examine how large life insurers are differentially exposed to the risk factors by running factor regressions at the firm level. Second, leveraging the extensive policy-level Firm Database, we estimate the hazard model to study the marginal effects of specific policy and policyholder characteristics on the relative risk. Third, we explore the heterogeneity in lapsation rates across geographies with different house price and employment experiences during the Great Financial Crisis.

4.2.1 Heterogeneity Across Firms

Table 4 presents the first set of results for large insurers. The table lists the 30 largest life insurers based on the in-force policy amounts at the end of 2020, which is the same group of life insurers that we used to construct the lapsation risk factors in Section 3.1. The third and the fourth column report the mean and the standard deviation of the historical lapse rates. The fifth column reports the correlation of the historical lapse rate series with the filtered employment series. The correlation coefficients are mostly negative, which is consistent with Figure 4. The sixth and the seventh column are the main results of interest: the exposures to the *Lapse Trend factor* and the *Lapse Cycle factor*. We note substantial variation in these risk exposures across companies. This suggests that optimal hedging strategies to manage lapsation risk vary across companies. The valuation impact of aggregate lapse risk also varies across companies.

4.2.2 Heterogeneity Across Policies

Table 5 presents the results using the policy-level data. The first column indicates the policy or policyholder characteristic that we examine. For the attained age and the policy size (death benefit amount in 2016 USD), we divide into groups and use the group indicator variables while omitting the oldest policyholder group and the largest policy group. The Risk Class (Better) variable indicates the initial risk classification of the policyholder by the life insurer at the time of underwriting, where the ultra preferred class takes +2, the select preferred class takes +1, the standard class takes 0, and the sub class takes -1 on the value within either Tobacco or Non-Tobacco risk ratings. The Shock Year variable is an indicator variable that takes on the value of one for term policies at maturity to capture the large spike in lapsation due to the renewability feature common in the U.S. term policy market.[8]

[8]See Figure 33 of Society of Actuaries and LIMRA (2019) for the effect of the shock year lapse "spikes". Both Society of Actuaries (2010) and Milliman (2020) provide detailed discussion on the shock year lapse effects. Instead of flagging both year T and year $T+1$ as in other source, we only flag year $T+1$ as the shock lapse year, because the Firm Database only records the policy status updates dates with about a 3-month delay. This is the same effect that we discuss in the baseline hazard rate graph.

Table 4. **Lapsation Risk Exposures to Lapse Trend and Cycle by Firm**

This table reports the lapsation risk exposures of large life insurers to the two lapsation risk factors. Specifically, we run the following regression:

$$Lapse\,Rate_t^j = \alpha^j + \beta^j_{Trend} Lapse\,Trend_t + \beta^j_{Cycle} Lapse\,Cycle_t + \varepsilon^j_t$$

where the superscript j represents the index for the 30 largest life insurer groups from the S&P Global Market Intelligence database.

Rank	Company Name	Mean Lapse	St. dev. Lapse	Corr. w. Employm.	Exposure to Lapse Trend	Exposure to Lapse Cycle
1	Prudential Financial Inc.	5.20	1.19	-0.39	1.08 (0.11)	0.94 (0.15)
2	Northwestern Mutual	3.74	0.35	-0.29	0.16 (0.05)	0.44 (0.06)
3	AIG	6.18	2.48	-0.06	1.68 (0.57)	1.39 (0.76)
4	Transamerica	7.48	1.18	-0.33	0.65 (0.26)	0.95 (0.34)
5	Lincoln Financial	6.02	1.36	-0.28	1.20 (0.21)	0.85 (0.28)
6	New York Life	5.90	0.75	-0.29	0.69 (0.12)	0.41 (0.16)
7	State Farm	6.36	0.98	-0.35	0.83 (0.09)	0.89 (0.12)
8	Protective	5.52	1.30	-0.05	1.06 (0.31)	0.26 (0.41)
9	Principal Financial Group Inc.	4.50	1.78	-0.45	1.65 (0.16)	1.37 (0.21)
10	MassMutual	4.83	0.76	-0.07	0.50 (0.15)	0.65 (0.19)
11	Legal & General U.S. only	4.75	0.98	-0.35	0.91 (0.11)	0.69 (0.15)
12	Primerica	9.97	1.50	-0.36	1.09 (0.16)	1.54 (0.21)
13	Genworth	5.28	1.23	-0.52	0.13 (0.39)	0.46 (0.51)
14	John Hancock	5.68	0.95	-0.52	0.59 (0.15)	0.98 (0.19)
15	Brighthouse Financial	5.77	1.35	-0.44	1.25 (0.23)	0.63 (0.31)
16	Pacific Life	6.31	1.58	-0.50	0.11 (0.38)	1.80 (0.50)
17	Allstate Corp	8.88	1.77	-0.34	1.50 (0.26)	1.32 (0.34)
18	Equitable Holdings	6.30	1.17	-0.29	1.27 (0.18)	0.25 (0.24)
19	MetLife	5.11	1.06	-0.18	0.98 (0.15)	0.65 (0.20)
20	USAA	2.57	0.34	0.01	0.20 (0.08)	0.22 (0.11)
21	Voya Financial Inc.	5.64	1.57	-0.29	1.41 (0.23)	1.01 (0.31)
22	Guardian	5.28	1.16	-0.34	1.17 (0.14)	0.64 (0.19)
23	Berkshire Hathaway Inc.	9.23	4.19	0.14	1.96 (1.28)	-0.35 (1.69)
24	Great-West U.S. only	6.32	2.36	-0.16	1.94 (0.52)	0.85 (0.70)
25	Sammons Enterprises Inc.	6.22	1.02	-0.28	0.89 (0.20)	0.44 (0.27)
26	KUVARE	6.72	1.76	-0.32	0.93 (0.36)	1.63 (0.48)
27	Zurich	8.25	1.47	-0.42	1.32 (0.19)	1.07 (0.25)
28	Nationwide	5.90	1.31	-0.44	1.10 (0.24)	0.77 (0.32)
29	Ohio National	5.85	0.66	-0.33	0.14 (0.21)	-0.20 (0.28)
30	Penn Mutual	5.29	1.30	-0.43	1.04 (0.21)	1.00 (0.27)

The second column reports the estimated coefficient β from fitting the Cox proportional hazard model specified in Equation (3). The third and the fourth columns report the standard error and the z score for each coefficient. The fifth column shows the standard deviation of each characteristic, where we use $\sigma_i = 1.0$ if characteristic z_i is a dummy variable. Since the lapse cycle factor has standard deviation 0.58 in our sample, we use $\sigma_{i,cycle} = \sigma_i \times 0.58$ for the interaction of characteristic z_i with the lapse cycle factor. The sixth column reports the marginal effect defined by $\beta_i \sigma_i$ for characteristic z_i.

Before we discuss the heterogeneous lapse cycle exposures, which is our main focus, we discuss the estimated baseline lapse rate. First, the signs of the un-interacted coefficients of attained age, gender, policy size, smoking, risk rating, term vs. whole and others characteristics are all consistent with the well-document patterns from the industry lapse experience, see for instance Society of Actuaries and LIMRA (2019) and Milliman (2020). Second, Figure 6 plots the estimated baseline hazard rate function $\lambda_0(\tau)$. The downward-sloping graph on policy age is consistent with the documented shape of the lapse term structure from the industry report (Society of Actuaries and LIMRA (2019)).[9]

We interpret the cyclical exposure of each characteristic based on the relative size of the marginal effect of the interacted variable compared to the marginal effect of the un-interacted lapse cycle variable. For example, the Risk Class (Better) $\times$ Lapse Cycle variable has the marginal effect of -0.03. Compared to the marginal effect of the un-interacted lapse cycle variable (-0.10), the effect is roughly 30% in magnitude. A policyholder with a better risk rating by one notch has 30% less cyclical lapse risk. We provide similar interpretations below.

The first split is by the attained age of the policyholder. The results show that, before retirement, younger policyholders have a much greater exposure to the lapse cycle factor. The second split shows that although male policyholders have higher lapse risk on average, the exposures to the *Lapse Cycle factor* is not significantly different from female policyholders.

Next, we look at smoker status and risk classification. Smokers and policyholders in a lower risk class (worse risks) have higher exposures to the *Lapse Cycle factor*. The marginal effects of smoking and a lower risk rating are about 10% and 30% of the un-interacted lapse cycle effect, respectively. Households with a poorer health arguably benefit most from the financial protection offered by life insurance, yet show the greatest propensity to lose their policy in a recession.

[9]There is a "kink" at the 2-year data point. This results from the operation of the Firm database, where it records the status update date for lapsation or surrender, not the last date of the coverage. In practice, there is usually a 30-day grace period to declare the lapsation, and there can be additional administrative delay of one to two months. With this limitation, many of "lapses" at the end of the first year are shifted by a few months and measured as the second-year lapse. Because this effect is common to all policies, the effect on β, the heterogeneous risk exposure, is minimal.

Table 5. **Lapsation Risk Exposures by Policy and Policyholder Characteristics**

This table reports the heterogeneous lapsation risk exposures of life insurance policies depending on various policy or policyholder characteristics. We estimate the following Cox proportional hazard model for policy j in the Firm Database issued at time t:

$$\lambda_{j,t+\tau} = \lambda_0(\tau) \exp(\boldsymbol{\beta}' \boldsymbol{Z}_{j,t+\tau})$$

where $\lambda_0(\tau)$ is the baseline hazard rate at policy age $\tau \geq 1$, and the log relative risk is linear in the vector of the policy or policyholder characteristics $\boldsymbol{Z}_{j,t+\tau}$.

Characteristic	β	SE	z	σ	Marginal Effect
Age Group 00-24	0.46	0.01	39.80	1.00	0.46
Age Group 25-34	0.46	0.01	50.51	1.00	0.46
Age Group 35-44	0.21	0.01	24.42	1.00	0.21
Age Group 45-54	0.17	0.01	19.05	1.00	0.17
Age Group 55-64	0.14	0.01	15.43	1.00	0.14
Age Group 00-24 x LapseCycle	0.34	0.02	17.11	0.58	0.19
Age Group 25-34 x LapseCycle	0.26	0.02	16.60	0.58	0.15
Age Group 35-44 x LapseCycle	0.29	0.02	18.82	0.58	0.17
Age Group 45-54 x LapseCycle	0.23	0.02	14.84	0.58	0.13
Age Group 55-64 x LapseCycle	0.11	0.02	6.58	0.58	0.06
Lapse Cycle	-0.18	0.02	-10.48	0.58	-0.10
Male	0.03	0.00	7.47	1.00	0.03
Male x LapseCycle	-0.01	0.01	-1.03	0.58	0.00
Size less than 100k	-0.30	0.01	-39.00	1.00	-0.30
Size 100k to 250k	0.10	0.01	17.00	1.00	0.10
Size 250k to 500k	0.07	0.01	11.80	1.00	0.07
Size 500k to 1mm	0.03	0.01	4.25	1.00	0.03
Size less than 100k x LapseCycle	-0.04	0.01	-3.49	0.58	-0.03
Size 100k to 250k x LapseCycle	-0.04	0.01	-3.82	0.58	-0.02
Size 250k to 500k x LapseCycle	-0.01	0.01	-1.38	0.58	-0.01
Size 500k to 1mm x LapseCycle	-0.01	0.01	-0.91	0.58	-0.01
Smoker	0.44	0.01	74.61	1.00	0.44
Smoker x LapseCycle	0.02	0.01	2.22	0.58	0.01
Risk Class (Better)	-0.20	0.00	-92.23	0.91	-0.18
Risk Class (Better) x LapseCycle	-0.04	0.00	-10.06	0.79	-0.03
Whole & Others	-0.12	0.00	-27.64	1.00	-0.12
Whole & Others x LapseCycle	0.14	0.01	20.37	0.58	0.08
Shock Year	1.79	0.02	85.97	1.00	1.79
Shock Year x LapseCycle	-0.89	0.04	-22.57	0.58	-0.51

Figure 6. **The Estimated Baseline Hazard Rate**

This figure plots the estimated baseline hazard rate from the Cox proportional hazard rate model using the Firm Database. The Cox proportional hazard model specifies that for policy j in the Firm Database issued at time t:

$$\lambda_{j,t+\tau} = \lambda_0(\tau) \exp(\boldsymbol{\beta}' \boldsymbol{Z}_{j,t+\tau})$$

where $\lambda_0(\tau)$ is the baseline hazard rate at policy age $\tau \geq 1$, and the log relative risk is linear in the vector of the policy or policyholder characteristics $\boldsymbol{Z}_{j,t+\tau}$.

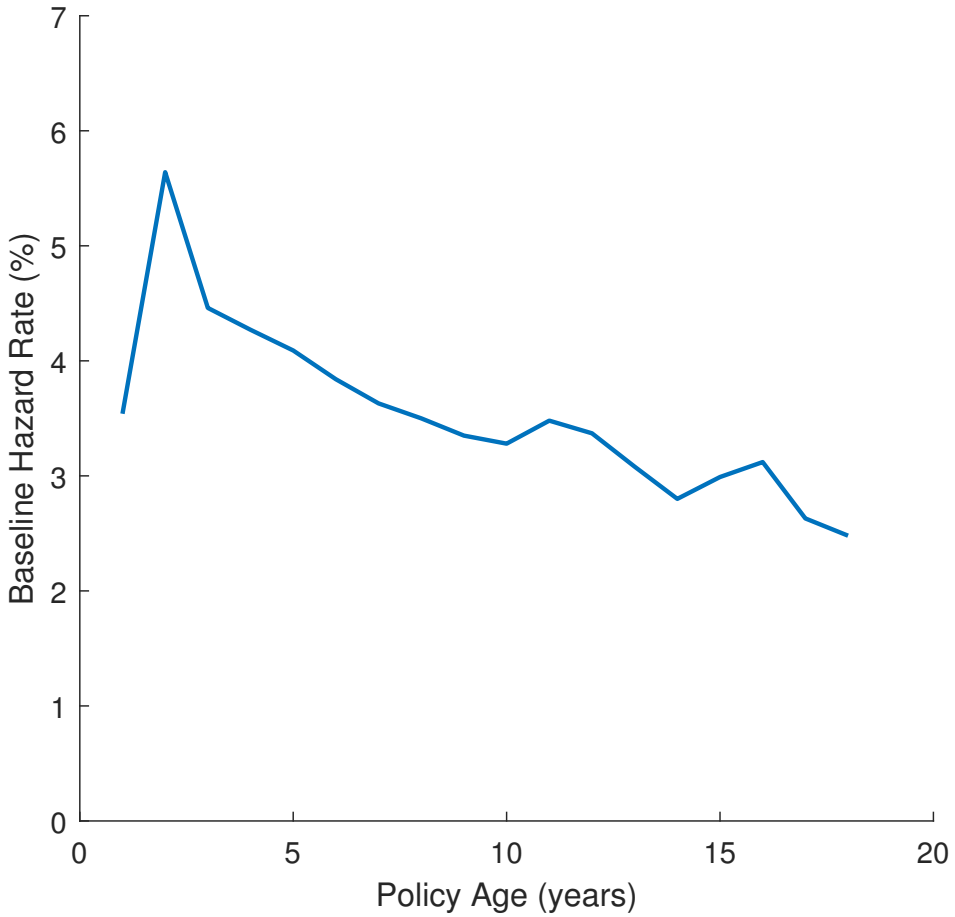

We then split the data by policy size (death benefit). Exposures to the lapse cycle increase modestly with policy size.

The last split of the data compares term policies to whole life policies and other policies such as variable or universal life policies. Lapse rates of whole and other life policies are more cyclical compared to term policies without cash surrender value. The magnitude of the additional cyclical exposure for the whole and other policies is about 80% of the uninteracted cyclical effect. If recessions cause a need for liquidity, for example because of an unemployment spell, whole life policyholders can surrender their policies thereby accessing the cash surrender value in these policies.

This rich pattern of heterogeneity in exposures suggests that there are important distributional consequences from aggregate lapsation risk. The fact that young and riskier policyholders are more likely to lapse their policy during economic downturns provides a new perspective on the costs of business cycles, in particular if households who lapse their policies are less likely to purchase a new policy in the future.

4.2.3 Geographical Heterogeneity During the 2008 Financial Crisis

Next, we explore the heterogeneity in lapsation rates across geographies during the 2008 financial crisis. Figure 7 presents the binscatter plots of the county-level lapse rate change, $(\Delta Lapse\,06-09)_c$, against the county-level economic variables during the Global Financial Crisis. The top panel plots the lapse rate change against the housing price change, $(\Delta HousingPrice\,06-09)_c$, and the bottom panel plots the lapse rate change against the unemployment change, $(\Delta Unemp\,06-09)_c$. The counties are sorted into 20 equal-sized bins based on the value of the economic variable on the horizontal axis. The blue dots are plotted at the equal-weighted averages for each bin and the orange dots are plotted at the weighted-averaged for each bin. The average in-force amount in 2006 is used to construct the weights, and the orange marker size indicates the bin-level sum of the weights. The blue lines show the OLS predictions while the orange lines show the weighted least squares (WLS) predictions. All three variables are winsorized at the 2.5% and 97.5% percentiles.

The top panel shows a clear negative relationship between the change in the lapse rate and house price changes, and the bottom panel shows a clear positive relationship between lapse rate changes and changes in the unemployment rate. Counties with more adverse housing and labor market conditions during the Great Financial Crisis experienced larger increases in the lapse rates.

We formalize this relationship by estimating county-level regressions. Table 6 presents the WLS results, which we prefer as the baseline specification. The OLS results are presented in Table A2 in the Appendix. Robust standard errors are reported. In Column (1) of Table

Figure 7. **Lapsation Rate Change vs. County-level Economic Variables**

This figure plots the lapsation change between 2006 and 2009 against the county-level economic variables. The top panel plots the lapsation rate change $((\Delta Lapse\,06-09)_c)$ against the housing price change $((\Delta HousingPrice\,06-09)_c)$ and the bottom panel plots the lapsation rate change $((\Delta Lapse\,06-09)_c)$ against the unemployment change $((\Delta Unemp\,06-09)_c)$. Counties are sorted into 20 equal-size bins based on the economic variable on the X-axis. The blue dots are plotted at the equal-weighted averages for each bin and the orange dots are plotted at the weighted-averaged for each bin. The average in-force amount in 2006 are used as the weights, and the orange marker size indicates the bin-level sum of the weights. The blue lines show the OLS predictions while the orange lines show the WLS predictions.

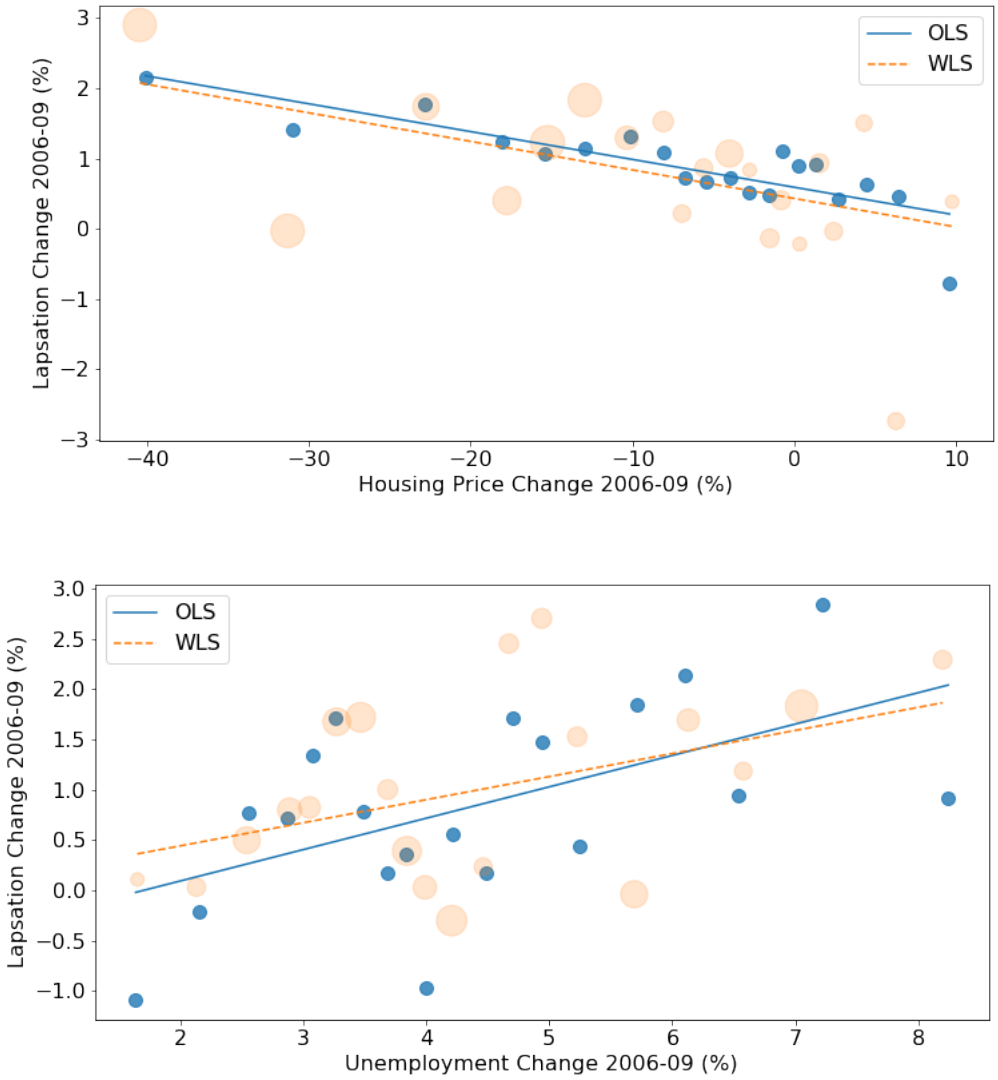

6, the point estimate on house price changes is -0.04 and it is statistically significant at the 5% level. The mean and standard deviation of $\Delta Housing\ Price\ 06-09$ are -7.8% and 12.5%, respectively, so that a one-standard deviation decline in house prices is associated with a 0.51% higher lapsation rate.

Similarly, in Column (4), the coefficient on the unemployment rate change is 0.23 and it is statically significant at the 5% level. The mean and standard deviation of $\Delta Unemp\ Rate\ 06-09$ are 4.4% and 1.7%, respectively, so that a one-standard deviation more severe unemployment rate increase is associated with a 0.39% higher lapsation rate.

In Columns (2) to (3) and (5) to (6), we control for median 2006 income[10] and 2006 log population. The coefficient on house price changes becomes more negative. Larger counties (usually in populous MSAs with higher median income) experienced more severe house price declines, but experienced a smaller increase in lapsation rates. Controlling for income and population thus makes the sensitivity of lapse rates to house prices larger. For unemployment changes, controlling for income and population does not affect the coefficient of interest much.

In Columns (7) to (9), we present the results when both house price changes and unemployment changes are included in the model. The effect from unemployment changes is subsumed by the coefficient on the house price change. The latter is still statistically significant at the 5% level, and is larger in absolute value than in Columns (1) to (3).[11]

In sum, regional variation in economic hardship correlates positively with lapsation rates, adding an additional dimension of heterogeneity to the results from the previous section, and adding evidence that policies tend to lapse more in adverse states of the world.

5 Valuation Model

In this section, we develop an asset pricing model to quantify the impact of aggregate lapsation risk on the valuation of life insurance policies. We calibrate the model to be consistent with asset pricing data. We then use the model to compute the mispricing and its impact on insurer profitability when insurance companies do not account for systematic lapsation risk in calculating insurance premiums.

[10] This is the imputed ACS income of 2006. If ACS data exists, we use the data, otherwise we use the predicted income of the following panel regression: $(ACSIncome)_{ct} = \beta * (HUDIncome)_{ct} + \alpha_c + \gamma_t$. The estimated β is ≈ 0.275.

[11] Comparing the WLS results in Table 6 to the OLS results in Table A2, the coefficients are similar in columns (1) to (6). When both house price change and unemployment rate change are included as regressors, the coefficients lose statistical significance, unlike in the WLS.

Table 6. **Lapse Rate Change against County-level Economic Variables: WLS**

This table reports the county-level regression of the change in lapse rates between 2006 and 2009 on the changes in economic variables between 2006 and 2009. We estimate the following cross-sectional regression:

$$(\Delta Lapse06-09)_c = \beta_0 + \beta_1 * (\Delta HousingPrice06-09)_c + \beta_2 * (\Delta Unemp06-09)_c + \gamma * X_c + \varepsilon_c$$

where county c is weighted by the average in-force amount in 2006. Robust standard errors are reported.

	Lapse Chg (1)	Lapse Chg (2)	Lapse Chg (3)	Lapse Chg (4)	Lapse Chg (5)	Lapse Chg (6)	Lapse Chg (7)	Lapse Chg (8)	Lapse Chg (9)
Δ Housing Price 06-09	-0.04058**	-0.04286***	-0.04782***				-0.04188**	-0.05265**	-0.05845**
	(0.01700)	(0.01649)	(0.01641)				(0.02135)	(0.02178)	(0.02271)
Δ Unemp 06-09				0.22959**	0.22791*	0.23695**	-0.01662	-0.11874	-0.12738
				(0.10811)	(0.11869)	(0.11364)	(0.13004)	(0.15784)	(0.15754)
ACS Income 2006		-0.00013	-0.00012		-0.00001	0.00000		-0.00018	-0.00017
		(0.00010)	(0.00010)		(0.00011)	(0.00011)		(0.00013)	(0.00012)
Log Population 2006			-0.00099*			-0.00033			-0.00102*
			(0.00060)			(0.00052)			(0.00061)
Constant	0.00431	0.01170*	0.02344***	-0.00017	0.00034	0.00371	0.00484	0.01820*	0.03073**
	(0.00262)	(0.00645)	(0.00906)	(0.00438)	(0.00966)	(0.01184)	(0.00416)	(0.01055)	(0.01437)
R^2	0.03301	0.03701	0.04198	0.01389	0.01390	0.01456	0.03311	0.03871	0.04395
Adj R^2	0.03174	0.03447	0.03819	0.01269	0.01150	0.01095	0.03055	0.03489	0.03888
N	762	762	762	823	823	823	759	759	759

Standard errors in parentheses

* p<0.1, ** p<0.05, *** p<0.01

5.1 Summary of the Economic Intuition

Before explaining the details of the model, we discuss the basic economic intuition for how aggregate lapsation risk affects the valuation of life insurance policies.

Let $\lambda_t = \mathbb{E}_t[Lapse_{t+1}]$ be the probability that a policyholder lapses her policy in the subsequent period, where $Lapse_{t+1}$ is one in case of lapsation and zero otherwise. In the presence of aggregate risk, the probability to be used in valuation accounts for the stochastic discount factor, $M^{\$}_{t+1}$:

$$\lambda^{Q}_t = \mathbb{E}_t\left[\frac{M^{\$}_{t+1}}{\mathbb{E}_t[M^{\$}_{t+1}]}Lapse_{t+1}\right] = \lambda_t + Cov_t\left(\frac{M^{\$}_{t+1}}{\mathbb{E}_t[M^{\$}_{t+1}]}, Lapse_{t+1}\right).$$

We have seen that lapsation is high during economic downturns, which coincides with periods when investors' marginal utility is high as well. The covariance term is therefore positive and the effective lapsation rate to be used for valuation, λ^{Q}, exceeds the actual lapsation rate, λ.

If an insurer ignores aggregate lapsation risk, then the lapsation rate used is too low. This has two opposing effects on the premium charged to policyholders. First, insurance companies pay a commission to insurance brokers to sell their products. If insurers use a lapsation rate that is too low, they understate the probability that the policy lapses before they have been able to recover the fixed cost of selling the policy. As a result, the premium charged is too low.

The opposing effect is a consequence of the fact that insurers charge a fixed premium during the term of the contract, while mortality rates increase. This implies that the first years of the contract are profitable (as the premium exceeds the costs of the mortality cover), and the later years of the contract are unprofitable (as the premium is lower than the costs of the mortality cover). If insurers use a lapsation rate that is too low, they put too much weight on the second part of the contract, and charge a premium that is too high.

A priori, it is unclear which effect dominates and how large these effects are, how they vary with the markup charged by the insurer, and with macroeconomic conditions such as the low-rate environment. To answer these questions, we develop a quantitative model in the remainder of this section.

5.2 Model Setup

The model builds on the affine valuation models that are widely used in finance, and we extend it to value life insurance policies in the presence of aggregate lapsation risk.

We assume that the $N \times 1$ vector of state variables, z_t, follows a Gaussian first-order VAR:

$$z_t = \mu + \Psi z_{t-1} + \Sigma^{\frac{1}{2}} \varepsilon_t, \tag{4}$$

with shocks $\varepsilon_t \sim i.i.d.\mathcal{N}(0, I)$ whose variance is the identity matrix, I. The companion matrix Ψ is an $N \times N$ matrix and $\Sigma^{\frac{1}{2}}$ is a lower-triangular matrix. As detailed below, the state vector contains a one-year government bond yield, the return on a credit portfolio, and the credit spread.

The nominal SDF $M^{\$}_{t+1} = \exp(m^{\$}_{t+1})$ is conditionally log-normal:

$$m^{\$}_{t+1} \;=\; -y^{\$}_{t,1} - \frac{1}{2}\Lambda_t'\Lambda_t - \Lambda_t'\varepsilon_{t+1}. \tag{5}$$

Note that $y^{\$}_{t,1} = -\mathbb{E}_t[m^{\$}_{t+1}] - 0.5\mathbb{V}_t[m^{\$}_{t+1}]$. The risk prices, Λ_t, are modeled as $\Lambda_t = \Lambda_0 + \Lambda_1 z_t$. We impose further restrictions on Λ_0 and Λ_1 below.

All lapsation rates λ are converted to log lapsation rates $\tilde{\lambda}$ satisfying $\exp(-\tilde{\lambda}) = 1 - \lambda$. We assume that the log lapsation factor is affine in the state vector, that is, $\tilde{l}_t = a_0 + a_1' z_t$. We parameterize the term structure of lapsation rates using the sequence of constants $\{b^{(n)}\}_{\forall n}$. The log lapsation rate of a policy of age n is then given by:

$$\tilde{\lambda}^{(n)}_t = b^{(n)}\tilde{l}_t,$$

with $b^{(n)} > 0$ and $b'^{(n)} < 0$.

Two comments are in order. First, the lapse rate can, in theory, become negative. However, the probability of this happening is so small that we favor this specification that provides a simple closed-form solution over more complicated alternatives. Second, the lapsation rate inherits the persistence of factors. We could generalize this by adding an additional component to the state variables in z_t that reflects an independent component in the lapsation rate.

5.3 Nominal Bonds

Given the assumptions we made, we can recursively find a closed-form solution for nominal bond yields.

Proposition 1. Nominal bond yields are affine in the state vector:

$$y^{\$}_t(\tau) = -\frac{A^{\$}_\tau}{\tau} - \frac{B^{\$\prime}_\tau}{\tau} z_t,$$

where the coefficients $A^{\$}_{\tau}$ and $B^{\$}_{\tau}$ satisfy the following recursions:

$$A^{\$}_{\tau+1} = A^{\$}_{\tau} + \frac{1}{2}\left(B^{\$}_{\tau}\right)' \Sigma \left(B^{\$}_{\tau}\right) + \left(B^{\$}_{\tau}\right)' \left(\mu - \Sigma^{\frac{1}{2}} \Lambda_0\right) \tag{6}$$

$$\left(B^{\$}_{\tau+1}\right)' = \left(B^{\$}_{\tau}\right)' \Psi - e'_{yn} - \left(B^{\$}_{\tau}\right)' \Sigma^{\frac{1}{2}} \Lambda_1, \tag{7}$$

initialized at $A^{\$}_0 = 0$ and $B^{\$}_0 = 0$.

Proof. See Appendix Section A.1. □

5.4 Term Life Policy

We now use the model to value term life policies. We consider a $T-$year term life insurance contract that is issued at time t. The annual mortality rate at age a is π_a, and it is typically increasing in age. The life insurance contract is sold via brokers and the broker compensation equals $C = \kappa p$, with p the insurance premium and κ a multiple of the annual premium. Hence, if $\kappa = 1$, then the broker receives one year of premiums.

For $\tau = 1, 2, \cdots, T$, the lapse rates $\{\lambda_{t+\tau}\}$ and the SDF $M^{\$}_{t+\tau}$ are modeled in Section 5.2. We denote the cumulative SDF by $M^{\$}_{t,1:\tau} = \prod_{s=1}^{\tau} M^{\$}_{t+s}$. The valuation equation for the life insurance policy equates the expected premium revenue with the expected cost of paying the broker and paying the death benefit to the policyholder:

$$\begin{aligned} & pE_t\left[1 + \sum_{\tau=1}^{T-1} M^{\$}_{t,1:\tau} \prod_{s=1}^{\tau}(1-\pi_{a+s-1}) \prod_{s=1}^{\tau}(1-\lambda^{(s)}_{t+s})\right] \\ & = C + (1+\phi)E_t\left[\sum_{\tau=1}^{T} M^{\$}_{t,1:\tau}\pi_{a+\tau-1} \prod_{s=1}^{\tau-1}(1-\pi_{a+s-1}) \prod_{s=1}^{\tau-1}(1-\lambda^{(s)}_{t+s})\right], \end{aligned}$$

where ϕ denotes the markup of the insurance policy before considering the brokerage fee.[12]

Using $C = \kappa p$, we can solve for the insurance premium:

$$p = (1+\phi)\frac{E_t\left[\sum_{\tau=1}^{T} M^{\$}_{t,1:\tau}\pi_{a+\tau-1} \prod_{s=1}^{\tau-1}(1-\pi_{a+s-1}) \prod_{s=1}^{\tau-1}(1-\lambda^{(s)}_{t+s})\right]}{E_t\left[1 + \sum_{\tau=1}^{T-1} M^{\$}_{t,1:\tau} \prod_{s=1}^{\tau}(1-\pi_{a+s-1}) \prod_{s=1}^{\tau}(1-\lambda^{(s)}_{t+s})\right] - \kappa}. \tag{8}$$

Given the assumptions made, we calculate a closed-form solution for $E_t\left[M^{\$}_{t,1:\tau} \prod_{s=1}^{\tau}(1-\lambda^{(s)}_{t+s})\right]$, which is the key term in computing the insurance premium. Note that the solution depends on the lapse factor exposures at different policy age, i.e. $b^{(1:\tau)} = \left\{b^{(1)}, b^{(2)}, \cdots, b^{(\tau)}\right\}$.

[12] Note that the timing is such that we first draw the health outcome (survival or death) and then proceed to the lapse decision. If this is reverse, the last term on the right-hand side would have $\prod_{s=1}^{t}(1-\lambda_s)$ instead of $\prod_{s=1}^{t-1}(1-\lambda_s)$.

We recursively solve for the two coefficient functions $P_\tau : \mathbb{R}^\tau \to \mathbb{R}$ and $Q_\tau : \mathbb{R}^\tau \to \mathbb{R}^N$ that satisfy $E_t\left[M^{\$}_{t,1:\tau}\prod_{s=1}^{\tau}(1-\lambda^{(s)}_{t+s})\right] = \exp\left(P_\tau(b^{(1:\tau)}) + Q_\tau(b^{(1:\tau)})' z_t\right)$. The other term $E_t\left[M_{t,1:\tau}\prod_{s=1}^{\tau-1}(1-\lambda^{(s)}_{t+s})\right]$ in the numerator can be calculated as a special case when $b^{(\tau)} = 0$, that is, if there is no lapsation in the final period. The following proposition provides the recursion for P_τ and Q_τ. Note that when $\tau = 0$, we slightly abuse the notation $P_\tau(b^{(2:\tau+1)}) = P_0$ and $Q_\tau(b^{(2:\tau+1)}) = Q_0$ for constants P_0 and Q_0 for simplicity.

Proposition 2. The term policy premium p can be written as:

$$p = (1+\phi)\frac{\sum_{\tau=1}^{T}\exp\left(P_\tau(b^{(1:\tau-1)},0) + Q_\tau(b^{(1:\tau-1)},0)' z_t\right)\pi_{a+\tau-1}\prod_{s=1}^{\tau-1}(1-\pi_{a+s-1})}{1+\sum_{\tau=1}^{T-1}\exp\left(P_\tau(b^{(1:\tau)}) + Q_\tau(b^{(1:\tau)})' z_t\right)\prod_{s=1}^{\tau}(1-\pi_{a+s-1}) - \kappa},$$

where the coefficient functions $P_\tau : \mathbb{R}^\tau \to \mathbb{R}$ and $Q_\tau : \mathbb{R}^\tau \to \mathbb{R}^N$ satisfy the following recursions:

$$\begin{aligned} P_{\tau+1}(b^{(1:\tau+1)}) &= -b^{(1)}a_0 + P_\tau(b^{(2:\tau+1)}) + \left(Q_\tau(b^{(2:\tau+1)}) - b^{(1)}a_1\right)'\left(\mu - \Sigma^{\frac{1}{2}}\Lambda_0\right) \\ &\quad + \frac{1}{2}\left(Q_\tau(b^{(2:\tau+1)}) - b^{(1)}a_1\right)'\Sigma\left(Q_\tau(b^{(2:\tau+1)}) - b^{(1)}a_1\right) \qquad (9) \\ \left(Q_{\tau+1}(b^{(1:\tau+1)})\right)' &= \left(Q_\tau(b^{(2:\tau+1)}) - b^{(1)}a_1\right)'\left(\Psi - \Sigma^{\frac{1}{2}}\Lambda_1\right) - e'_{yn}, \qquad (10) \end{aligned}$$

initialized at $P_0 = 0$ and $Q_0 = 0$.

Proof. See Appendix Section A.2. □

The recursion in Proposition 2 can be regarded as an extension of the recursion in Proposition 1. When lapse rates do not depend on the state of the economy, i.e. $b^{(1)} = b^{(2)} = \cdots = b^{(\tau)} = 0$, $E_t\left[M^{\$}_{t,1:\tau}\prod_{s=1}^{\tau}(1-\lambda^{(s)}_{t+s})\right]$ simplifies to the nominal bond price of maturity τ. We verify that $P_\tau(\vec{0}) = A^{\$}_\tau$ and $Q_\tau(\vec{0}) = B^{\$}_\tau$. Indeed, Equations (9) and (10) are equivalent to Equations (6) and (7) when $b^{(1)} = b^{(2)} = \cdots = b^{(\tau+1)} = 0$.

5.5 Calibration

We calibrate the model using financial market data at an annual frequency. Instead of directly estimating the VAR model presented in Section 5.2 on annual data, we specify an underlying monthly VAR model. We estimate the monthly model, properly time-aggregated to match moments obtained from annual financial market data. The advantage of this modeling and calibration approach is that it allows us to simultaneously capture the dependency

of the lapse rates on the average of financial market state variables during the year and the relationship between the credit risk premium and the credit spread at the end of the year.[13]

The three-dimensional state vector $z_t = (r_t, cr_t, s_t)'$ contains the 1-year Constant Maturity U.S. Treasury rate (GS1 in FRED), the monthly credit return calculated from the ICE BofA BBB US Corporate Index Total Return Index (BAMLCC0A4BBBTRIV in FRED) and the credit spread, defined as Moody's Seasoned Baa Corporate Bond Yield Relative to Yield on 10-Year Treasury Constant Maturity (BAA10Y in FRED) for the sample period 1990–2020. We convert the interest rate, credit return, and credit spread into logarithms before estimating the VAR model. The monthly specification is the same as Equation (4) with the monthly VAR parameters $(\mu, \Psi, \Sigma^{\frac{1}{2}})$:

$$z_t = \mu + \Psi z_{t-1} + \Sigma^{\frac{1}{2}} \varepsilon_t, \tag{11}$$

The monthly dynamics imply the following annual dynamics:

$$z_{t+k} = \left(\sum_{i=0}^{k-1} \Psi^i \right) \mu + \Psi^k z_t + \sum_{i=0}^{k-1} \Psi^i \Sigma^{\frac{1}{2}} \varepsilon_{t+k-i}, \tag{12}$$

and

$$\sum_{k=1}^{K} z_{t+k} = \sum_{k=1}^{K} \left(\sum_{i=0}^{k-1} \Psi^i \right) \mu + \sum_{k=1}^{K} \Psi^k z_t + \sum_{k=1}^{K} \sum_{i=0}^{k-1} \Psi^i \Sigma^{\frac{1}{2}} \varepsilon_{t+k-i}. \tag{13}$$

Equation (12) describes the dynamics of the annually-sampled interest rate and the credit spread (r_{t+12} and s_{t+12}). Equation (13) describes the annual log holding period return on the credit portfolio, which is the sum of twelve monthly log returns ($\sum_{k=1}^{12} cr_{t+k}$). Equation (13) multiplied by 1/12 also describes the dynamics of the state variables, averaged over the year. It is those averages that drive the lapsation behavior.

The monthly nominal SDF $M^{\$}_{t+1} = \exp(m^{\$}_{t+1})$ is given by:

$$m^{\$}_{t+1} = -\frac{\delta_0}{12} - \frac{\delta_1' z_t}{12} - \frac{1}{2} \Lambda_t' \Lambda_t - \Lambda_t' \varepsilon_{t+1}, \tag{14}$$

where the one-month discount rate $y^{\$}_{t,1} = \frac{\delta_0}{12} + \frac{\delta_1' z_t}{12}$ is an affine function of the state variable z_t. We parameterize the market price of risk Λ_t as:

$$\Lambda_t = \Lambda_0 + \Lambda_1 z_t = \Lambda_0 + \hat{\Lambda}_1 e_3' z_t,$$

[13] Lapsation rate data are available only at the annual frequency. When we model and estimate (in Table 3) the relationship between the annual lapse rates and the financial market state variables, the lapse rate depends on the average state variables throughout the year not just on the end-of-year state variables. Using a monthly VAR allows us to model the annual lapse rate as a function of the 12-month average of monthly state variables.

which requires us to identify three parameters, two for $\Lambda_0 = (\Lambda_0^r, \Lambda_0^{cr}, 0)'$ and one for $\hat{\Lambda}_1 = (0, \zeta, 0)'$.

We use the following three moments to calibrate these three market price of risk parameters. First, we match the average slope of the yield curve, defined as the difference between the 10- and 1-year Treasury bond yields. Second, we match the unconditional credit risk premium. Third, we match the linear dependence of the credit risk premium on the lagged credit spread. Additionally, (δ_0, δ_1) are estimated from the restriction that the one-year risk-free interest rate implied by the monthly SDF equals the one-year bond yield included in the state vector, r_t.

Specifically, we model the monthly excess return on the credit portfolio as:

$$cr_{t+1} - y_{t,1}^{\$} = \gamma_0 + \gamma_1 s_t + \sigma^{cr} e_{t+1},$$

with $e_{t+1} \sim \mathcal{N}(0,1)$, so that the expected excess return depends on the credit spread:

$$E_t[cr_{t+1}] - y_{t,1}^{\$} = \gamma_0 + \gamma_1 s_t.$$

The Euler equation for the credit portfolio then implies:

$$E_t[cr_{t+1}] + \frac{1}{2} V_t[cr_{t+1}] - y_{t,1}^{\$} = -Cov_t[cr_{t+1}, m_{t+1}^{\$}]$$

Using our assumption on the credit return and the affine structure of the SDF, this can be rewritten as:

$$\gamma_0 + \gamma_1 s_t + \frac{1}{2}(\sigma^{cr})^2 = \Lambda_0^r \sigma^{cr} Cov_t[e_{t+1}, \varepsilon_{t+1}^r] + (\Lambda_0^{cr} + \zeta s_t)\sigma^{cr} Cov_t[e_{t+1}, \varepsilon_{t+1}^{cr}]$$

Matching the unconditional credit risk premium delivers the second moment condition:

$$\gamma_0 + \gamma_1 E[s_t] + \frac{1}{2}(\sigma^{cr})^2 = \Lambda_0^r \sigma^{cr} Cov[e_{t+1}, \varepsilon_{t+1}^r] + (\Lambda_0^{cr} + \zeta E[s_t])\sigma^{cr} Cov[e_{t+1}, \varepsilon_{t+1}^{cr}] \tag{15}$$

and matching the conditional credit spread delivers the third moment condition:

$$\gamma_1 = \zeta \sigma^{cr} Cov[e_{t+1}, \varepsilon_{t+1}^{cr}] \tag{16}$$

Appendix B contains the details of the calibration process. The estimated monthly dy-

namics that result from matching moments measured in annual data are as follows:

$$\begin{bmatrix} r_{t+1} \\ cr_{t+1} \\ s_{t+1} \end{bmatrix} = \begin{bmatrix} 0.0006 \\ -0.0139 \\ 0.0026 \end{bmatrix} + \begin{bmatrix} 0.9792 & 0 & 0 \\ 0.0933 & 0 & 0.7245 \\ 0 & 0 & 0.8888 \end{bmatrix} \begin{bmatrix} r_t \\ cr_t \\ s_t \end{bmatrix} + \begin{bmatrix} 0.0041 & 0 & 0 \\ 0.0013 & 0.0242 & 0 \\ -0.0023 & -0.0025 & 0.0016 \end{bmatrix} \begin{bmatrix} \varepsilon^r_{t+1} \\ \varepsilon^{cr}_{t+1} \\ \varepsilon^s_{t+1} \end{bmatrix}$$

The estimated market price of risks are $\Lambda^r_0 = -0.1265$, $\Lambda^{cr}_0 = -0.5365$ and $\zeta = 29.98$. We verify that the model indeed matches the unconditional slope of the log yield curve of 1.36% and the unconditional credit risk premium of 4.43% (equivalently, the monthly unconditional credit risk premium of 0.41%), as well as the observed dependence of the annual credit risk premium on the 12-month lagged credit spread.

Next, we calibrate the parameters for the aggregate lapsation process, modeled as follows,

$$\begin{aligned} \tilde{l}_t &= a_0 + a_1' \bar{z}_t, \\ \tilde{\lambda}^{(n)}_t &= b^{(n)} \tilde{l}_t, \end{aligned}$$

where $\bar{z}_t$ denotes the 12-month moving average of the state variables. We first calibrate the parameters a_0 and a_1. By regressing the log lapsation rate $\tilde{l}_t$ on a constant, the constant-maturity U.S. Treasury 10-year log rate ($y^{\$}_{10,t}$), and the Baa-10y log spread (s_t) over the period 2000 to 2020 (annual average financial market data), we obtain the following relationship: $\tilde{l}_t = 0.0094 + 0.85 y^{\$}_{10,t} + 0.94 s_t$. Using the theoretical relationship $y^{\$}_{10,t} = 0.02986 + 0.41247 r_t$ from the calibrated yield curve, we obtain the coefficients $a_0 = 0.0347$ and $a_1 = (0.35, 0, 0.94)'$.

We calibrate the term structure of lapsation coefficients $\{b^{(n)}\}$ by parameterizing $\{b^{(n)}\} = u + \dfrac{v}{n+w}$, and we search for the vector (u, v, w) that delivers the closest fit for the 2007-2009 and 2009-2013 lapsation term structures to the term policy lapsation curves observed in the data (Society of Actuaries and LIMRA, 2012, 2019).[14] The calibrated term structure is $b^{(n)} = 0.54 + \dfrac{1.75}{n + 0.75}$ and the model-implied lapsation term structure is reasonably close to the data, as shown in Figure 8.

Figure 9 presents the historical paths of the model state variables, and the model-implied lapse rates and the market price of risks. In the top panel, we plot the first and the third state variables (r_t, s_t) retrieved from FRED between 2000 and 2020. The middle panel compares the actual lapse rate data with the model-implied lapse rates, showing that our lapsation

[14] We do not model the extendibility of a term life policy and the associated "shock lapses" at the end of the level premium periods, so we calculate the 6-10 and 11-20 average lapse rates excluding the policy ages affected by the shock lapses (10, 11, 15, 16, 20). See Society of Actuaries (2010) for a detailed investigation of the shock lapses after the level-premium period. The report shows that most of the shock lapses are occurring at the end of the policy age T and the beginning of the policy age $T + 1$.

Figure 8. **Lapse Rate Calibration**

This figure plots the calibrated lapse rates from the model and compare it to the Data for 2007-2009 and 2009-2013 periods (Society of Actuaries and LIMRA, 2012, 2019). See Section 5.5 for the details of the calibration process.

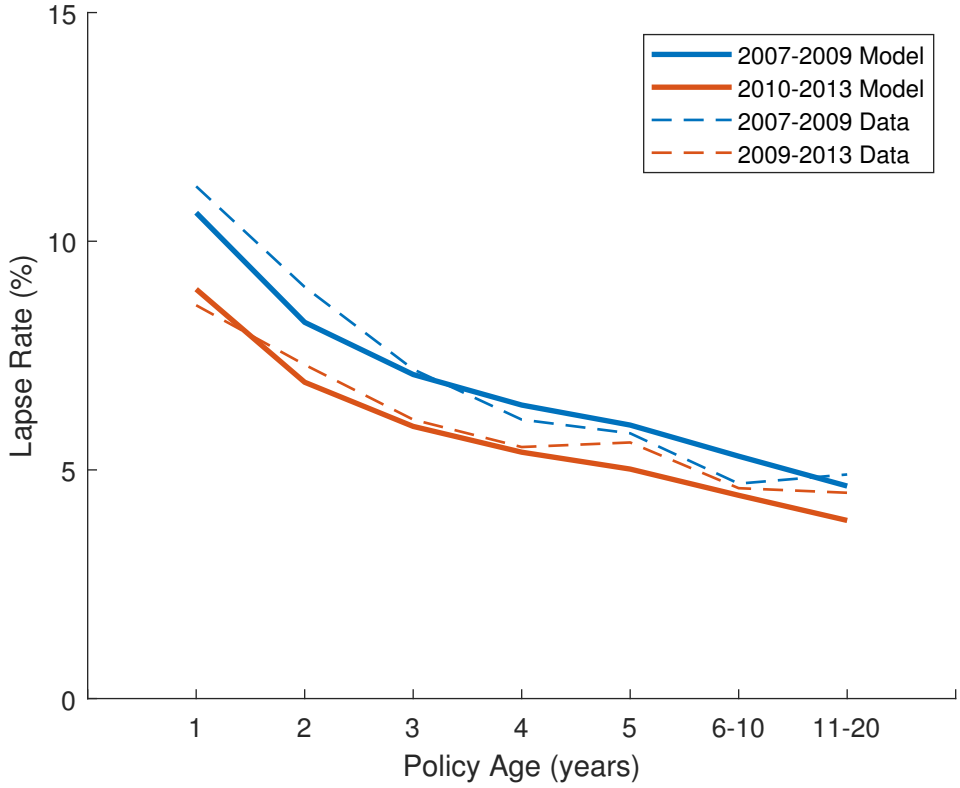

Figure 9. **Lapsation Model and Data**

The top panel plots the historical paths of two state variables, (r_t, s_t), of the asset pricing model. The middle panel compares the actual lapse rate data with the model-implied lapse rates. For the details of model calibration, see Section 5.5. The bottom panel plots the model-implied market price of risk.

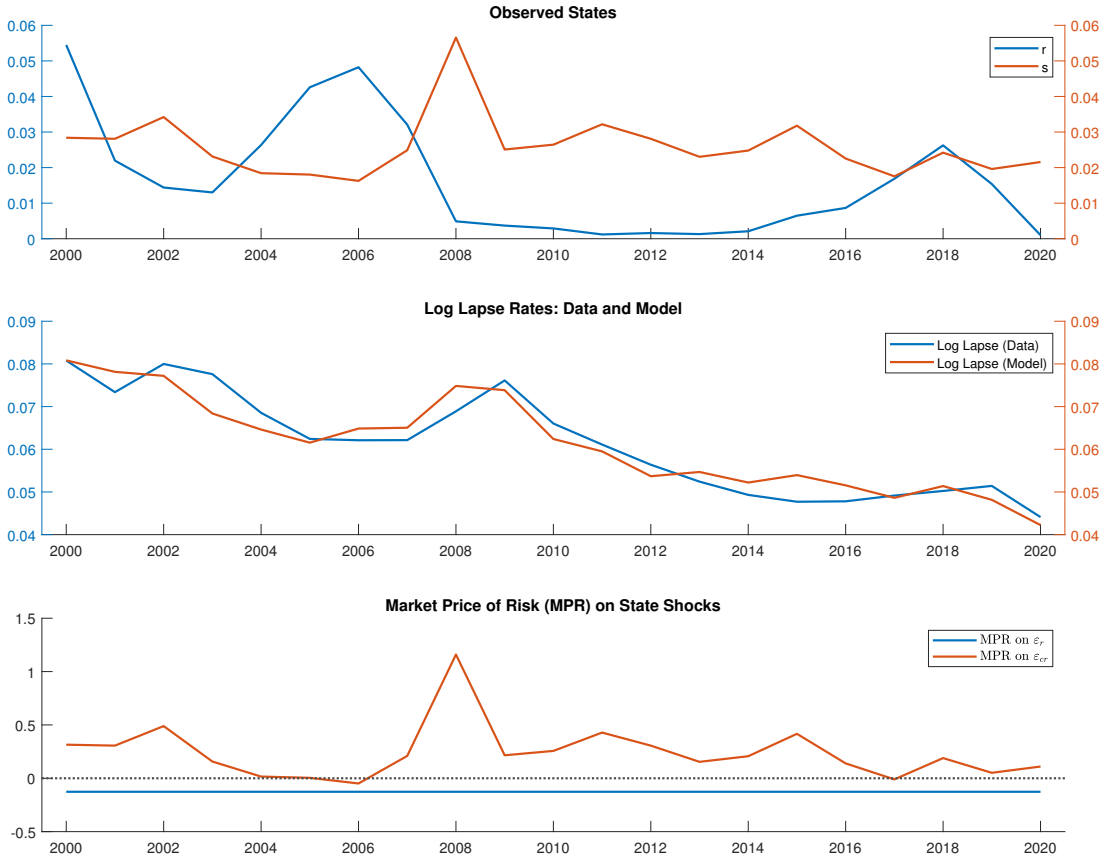

model provides a good fit. The bottom panel shows the time variation in the market price of risk on the credit return shock (the market price of risk on the interest rate shock is constant). During the Great Financial Crisis when the credit spread was high, the market price of credit risk was high, and lapsation was high. It is this positive covariance between lapsation rates and marginal utility that is the key new ingredient in our insurance pricing model.

5.6 Life Insurance Mispricing when Ignoring Aggregate Lapsation Risk

We now study an insurer who does not consider systematic lapsation risk when pricing life insurance contracts. We first consider the correct premium when the life insurer properly

accounts for aggregate lapsation risk. We repeat Equation (8) for convenience:

$$p = (1+\phi)\frac{E_t\left[\sum_{\tau=1}^{T} M^{\$}_{t,1:\tau}\pi_{a+\tau-1}\prod_{s=1}^{\tau-1}(1-\pi_{a+s-1})\prod_{s=1}^{\tau-1}\exp(-\tilde{\lambda}^{(s)}_{t+\tau})\right]}{E_t\left[1+\sum_{\tau=1}^{T-1} M^{\$}_{t,1:\tau}\prod_{s=1}^{\tau}(1-\pi_{a+s-1})\prod_{s=1}^{\tau}\exp(-\tilde{\lambda}^{(s)}_{t+\tau})\right]-\kappa}.$$

The correct expected profit to the insurer V is:

$$\begin{aligned}
V^{correct} &= p\cdot\left(\underbrace{E_t\left[1+\sum_{\tau=1}^{T-1} M^{\$}_{t,1:\tau}\prod_{s=1}^{\tau}(1-\pi_{a+s-1})\prod_{s=1}^{\tau}\exp(-\tilde{\lambda}^{(s)}_{t+\tau})\right]}_{=\alpha(T)}-\kappa\right)\\
&\quad-\underbrace{E_t\left[\sum_{\tau=1}^{T} M^{\$}_{t,1:\tau}\pi_{a+\tau-1}\prod_{s=1}^{\tau-1}(1-\pi_{a+s-1})\prod_{s=1}^{\tau-1}\exp(-\tilde{\lambda}^{(s)}_{t+\tau})\right]}_{=\beta(T)}\\
&= p\cdot(\alpha(T)-\kappa)-\beta(T)\\
&= \phi\beta(T),
\end{aligned}$$

where we have a closed-form solution for $\alpha(T) = 1+\sum_{\tau=1}^{T-1}\exp\left(P_\tau(b^{(1:\tau)})+Q_\tau(b^{(1:\tau)})'z_t\right)\prod_{s=1}^{\tau-1}(1-\pi_{a+s-1})$ and $\beta(T) = \sum_{\tau=1}^{T}\exp\left(P_\tau(b^{(1:\tau-1)},0)+Q_\tau(b^{(1:\tau-1)},0)'z_t\right)\pi_{a+\tau-1}\prod_{s=1}^{\tau-1}(1-\pi_{a+s-1})$.[15]

Intuitively, $\alpha(T)$ measures the number of years of premium income the insurer can expect to receive in the presence of lapsation risk and mortality risk. The first arrival of either lapsation or policyholder death ends the premium revenue claim. $\beta(T)$ measures the expected value of a \$1 death benefit pay-out from the perspective of the insurer. This death benefit only needs to be paid out if the policyholder dies during the term of the life insurance contract and the policy did not yet lapse.

We contrast this case with the case where an insurer ignores the covariance between the SDF and lapsation when pricing the term life insurance contract. To capture this scenario, we assume that the lapse rate depends on an independent lapsation factor, which is defined as $\tilde{l}^{ind}_t = a_0 + a_1'\bar{z}^{ind}_t$. The independent state vector z^{ind}_t follows the process $z^{ind}_{t+1} = \mu + \Psi z^{ind}_t + \Sigma^{\frac{1}{2}}\tilde{\varepsilon}_{t+1}$ with shocks $\tilde{\varepsilon}_t \sim N(0,I)$ that are independent from ε_t. This modeling approach preserves the distribution of lapsation rates, while decoupling lapsation risk from shocks to the SDF.

When both $\alpha(T)$ and $\beta(T)$ are incorrectly calculated based on this independent lapsation

[15] See Appendix B.3 for details on the calculation of the terms in mispricing formula such as $\alpha(T), \beta(T), \tilde{\alpha}(T), \tilde{\beta}(T)$.

model, denoted by $\tilde{\alpha}(T)$ and $\tilde{\beta}(T)$, respectively, the premium is set as $\tilde{p} = (1+\phi)\frac{\tilde{\beta}(T)}{\tilde{\alpha}(T)-\kappa}$. We can calculate $\tilde{\alpha}(T)$ and $\tilde{\beta}(T)$ also in closed form as $\tilde{\alpha}(T) = 1 + \sum_{\tau=1}^{T-1} L_\tau Z_\tau \prod_{s=1}^{\tau-1}(1-\pi_{a+s-1})$ and $\tilde{\beta}(T) = \sum_{\tau=1}^{T} L_{\tau-1} Z_\tau \pi_{a+\tau-1} \prod_{s=1}^{\tau-1}(1-\pi_{a+s-1})$ for $Z_\tau = E_t\left[M^{\$}_{t,t+1:t+\tau}\right]$ and $L_\tau = E_t\left[\prod_{s=1}^{\tau}(1-\lambda^{(s)}_{t+s})\right]$. Appendix A.2 and Section B.3 contains the affine recursions for L_τ and Z_τ.

When the premium $\tilde{p}$ is charged, but actual lapsation is subject to aggregate risk, the insurer's profit is given by:

$$\begin{aligned} V^{realized} &= \tilde{p}\cdot(\alpha(T)-\kappa) - \beta(T) \\ &= (1+\phi)\left(\frac{\alpha(T)-\kappa}{\tilde{\alpha}(T)-\kappa}\right)\tilde{\beta}(T) - \beta(T). \end{aligned}$$

We measure the impact of ignoring aggregate priced risk on the life insurer's profits as $Mispricing(\%) = \frac{V^{realized}-V^{correct}}{V^{correct}}$. We first study the numerator of this expression:

$$\begin{aligned} V^{realized} - V^{correct} &= (1+\phi)\left(\frac{\alpha(T)-\kappa}{\tilde{\alpha}(T)-\kappa}\right)\tilde{\beta}(T) - \beta(T) - \phi\beta(T) \\ &= (1+\phi)\left(\frac{\alpha(T)-\kappa}{\tilde{\alpha}(T)-\kappa} - 1\right)\tilde{\beta}(T) + (1+\phi)\left(\tilde{\beta}(T)-\beta(T)\right) \end{aligned}$$

We find that $\alpha(T) < \tilde{\alpha}(T)$ and $\beta(T) < \tilde{\beta}(T)$. Intuitively, lapse rates tend to increase during bad times (high SDF states). Taking this covariance into account shortens the duration of the premium leg and lowers the expected discounted death benefit payment. The effect of aggregate lapsation risk is to increase the effective lapse rates. The risk-neutral lapse rates (under the $\mathbb{Q}$ measure) are higher than the physical lapse rates (under the $\mathbb{P}$ measure).

We use the notation $\tilde{\alpha}(T)/\alpha(T) = 1+\Delta_{\alpha,T}$ and $\tilde{\beta}(T)/\beta(T) = 1+\Delta_{\beta,T}$ for $\Delta_{\alpha,T}, \Delta_{\beta,T} > 0$. Then, after dividing the previous expression by $V^{correct}$ and some algebraic manipulation, we can express the Mispricing(%) measure as the sum of two components:

$$\begin{aligned} Mispricing(\%) &= \frac{V^{realized}-V^{correct}}{V^{correct}} \\ &= \underbrace{(1+\phi^{-1})\left(\frac{\Delta_{\alpha,T}}{1+\Delta_{\alpha,T}} - \frac{\Delta_{\alpha,T}}{1+\Delta_{\alpha,T}-\kappa/\alpha(T)}\right)(1+\Delta_{\beta,T})}_{=Fixed-Cost\,Effect<0} \\ &\quad + \underbrace{(1+\phi^{-1})\left(\frac{\Delta_{\beta,T}}{1+\Delta_{\beta,T}} - \frac{\Delta_{\alpha,T}}{1+\Delta_{\alpha,T}}\right)(1+\Delta_{\beta,T})}_{=Mortality\,Effect>0} \end{aligned} \tag{17}$$

The fixed-cost effect term shows how the presence of the broker cost ($\kappa > 0$) affects our

mispricing measure. The insurer has to pay the fixed cost when the policy is underwritten. Early lapsation means that the insurer may not earn enough premium income to offset the cost of the broker fee. The higher the lapsation rate, the stronger the detrimental effect of fixed costs on profits. Since the effective lapsation rate is higher when accounting for priced aggregate lapsation risk, the fixed-cost effect is negative. In other words, not correctly considering systematic lapsation risk leads insurers to earn too little profit.

The second term is labeled a mortality effect because the sign of the term is determined by the relative size of $\Delta_{\beta,T}$ and $\Delta_{\alpha,T}$. We observe $\Delta_{\beta,T} > \Delta_{\alpha,T}$ in our calibration when mortality rises with age. With a flat mortality curve, $\Delta_{\alpha,T} \approx \Delta_{\beta,T}$ and mispricing captures mostly the fixed-cost effect. However, under a realistic mortality curve, the mortality rate exponentially rises in age and $\Delta_{\beta,T} >> \Delta_{\alpha,T}$. The mortality effect contributes positively to the mispricing measure. Intuitively, the insurer charges a flat premium throughout the life of the contract. The expected cost, by contrast, increases with age as mortality rates increase. Putting the fixed cost aside, the insurer experiences profits during the early years (as the flat premium exceeds the costs of mortality coverage) and losses during the later years of the contract (as the flat premium is lower than the costs of mortality coverage). If the insurer understates lapsation risk, it puts more weight on the later years during which the insurer experiences losses. As a result, the premium is set too high and the insurers unexpectedly earns excess profits.

Because the mispricing decomposition shows two countervailing effects, we need to quantitatively assess the relative magnitude of the two effects. We do so for a hypothetical 40 year-old male policyholder with a realistic mortality curve.[16] The fee paid to the broker is known to be between 50% to 100% of the first-year premium revenue, so we use $\kappa = 0.5, 0.75$, and 1.0, with benchmark value $\kappa = 0.75$. We vary the margin parameter ϕ in a reasonable range by using values $\phi = 0.05, 0.1, 0.2$. In Appendix C we test the validity of the markup assumption by calculating the insurer's expected share θ from the underwriting profit, after paying the broker's share $(1 - \theta)$. The 40% to 50% profit share range for term policies ranging from 10 to 20 years in maturity (see Table A1) in our baseline cases $\phi = 10\%$ and $\kappa = 0.75$ is in line with our understanding of the broker fee structure in the market.

Table 7 reports the mispricing measure and its decomposition. We find that the mortality effect dominates the fixed-cost effect, so that insurers who ignore priced aggregate lapsation risk earn excess profits. In our baseline case, $\kappa = 0.75$ and $\phi = 10\%$, the realized profit for a 10-year term policy is 6.9% higher than the theoretically correct one. This mispricing is decomposed into the two effects previously discussed in the second and third panels of the

[16] We use the 2017 Loaded CSO (Commissioners Standard Ordinary) Composite mortality table (https://www.soa.org/resources/experience-studies/2015/2017-cso-tables). We use the select mortality table to reflect the fact that insurers in practice are able to select policyholders with lower-than-population mortality risk, at least in the early years of the policy.

table. The insurer has to pay 75% of the first year premium to the brokers as a fixed cost. Ignoring the accelerated lapsation during recessions (higher lapsation under $\mathbb{Q}$) results in 3.2% understatement of the profit. On the other hand, the insurer charges a higher premium than the theoretically correct one (0.6% higher premium before markup and fixed-costs), as she is pricing a higher likelihood of having to pay out the death benefit when she assumes that lapsation rates are lower (under $\mathbb{P}$ than under $\mathbb{Q}$). The mortality effect makes the realized profit 10.0% higher compared to the correct profit. Since the mortality effect outweighs the fixed-cost effect, ignoring systematic lapsation risk in pricing decisions results in an excess profit of 6.9% compared to the case where the insurer correctly considered systematic lapsation risk. Term life policies would be cheaper in the world with correct pricing and profits would be lower.

The mispricing effect increases strongly in the maturity of the policy. The excess profit is 29.3% for a 20-year policy, due to a much stronger mortality effect. The reason is that mortality rises exponentially in age, and is much higher around age 60 than around age 40. This backloading of mortality risk interacts with lapsation risk. Understating lapsation risk in the incorrect pricing model results in a much higher expected death benefit payout than in the correct pricing model. The incorrect insurer charges a much higher premium and earns much higher profits. We have verified that with a (counter-factually) flat mortality rate profile, the mortality effect remains near zero for the 20-year policy.

Mispricing falls in both κ and ϕ. A higher fixed cost κ, while holding the markup ϕ fixed, results in a lower fixed-cost effect while the mortality effect is not changed. As the markup ϕ increases, holding κ fixed, both the fixed-cost effect and the mortality effect decline due to the $1 + \phi^{-1}$ term in Equation (17).

5.7 Using Corporate Bond Yields to Value Life Insurance Policies

Life insurers can use a corporate credit curve when calculating discounted present values for reserve calculations (National Association of Insurance Commissioners, 2021). The stated argument is that life insurers mostly hold corporate bonds on their balance sheet. This argument is incorrect because what a firm holds on the asset side should not affect the valuation of its liabilities. The premature death risk of individual policyholders is idiosyncratic, thus payouts on a portfolio of such policies should be discounted with the Treasury yield curve, not the corporate credit curve. As we have shown above, lapsation is correlated with corporate credit risk, and this affects valuations of life insurance contracts. These effects should be modeled via the covariation of lapsation rates and the SDF, and not as an ad-hoc adjustment to discount rates.

We investigate whether the observed credit-curve discounting practice mitigates the mis-

Table 7. **Mispricing of Term Life Policies without Aggregate Lapse Risk**

This table presents the calculated mispricing measure defined in Section 5.6 by

$$Mispricing(\%) = \frac{V^{realized} - V^{correct}}{V^{correct}}$$

where $V^{correct} = \phi\beta(T)$ is the correct profit of selling the term policy at markup ϕ assuming the correct pricing, and $V^{realized} = \tilde{p} \cdot (\alpha(T) - \kappa) - \beta(T)$ is the realized valuation based on the incorrect pricing when the aggregate lapsation risk is ignored.

Mispricing (%)				
		κ=0.5	κ=0.75	κ=1.0
10-year Term Policy	ϕ= 5%	15.3%	13.1%	10.7%
	ϕ= 10%	8.0%	6.9%	5.6%
	ϕ= 20%	4.4%	3.7%	3.1%
15-year Term Policy	ϕ= 5%	34.3%	31.6%	28.8%
	ϕ= 10%	18.0%	16.6%	15.1%
	ϕ= 20%	9.8%	9.0%	8.2%
20-year Term Policy	ϕ= 5%	59.0%	56.0%	52.8%
	ϕ= 10%	30.9%	29.3%	27.7%
	ϕ= 20%	16.9%	16.0%	15.1%
Fixed-Cost Effect (%)				
		κ=0.5	κ=0.75	κ=1.0
10-year Term Policy	ϕ= 5%	-3.9%	-6.0%	-8.4%
	ϕ= 10%	-2.0%	-3.2%	-4.4%
	ϕ= 20%	-1.1%	-1.7%	-2.4%
15-year Term Policy	ϕ= 5%	-4.8%	-7.4%	-10.3%
	ϕ= 10%	-2.5%	-3.9%	-5.4%
	ϕ= 20%	-1.4%	-2.1%	-2.9%
20-year Term Policy	ϕ= 5%	-5.5%	-8.5%	-11.7%
	ϕ= 10%	-2.9%	-4.5%	-6.1%
	ϕ= 20%	-1.6%	-2.4%	-3.3%
Mortality Effect (%)				
		κ=0.5	κ=0.75	κ=1.0
10-year Term Policy	ϕ= 5%	19.1%	19.1%	19.1%
	ϕ= 10%	10.0%	10.0%	10.0%
	ϕ= 20%	5.5%	5.5%	5.5%
15-year Term Policy	ϕ= 5%	39.1%	39.1%	39.1%
	ϕ= 10%	20.5%	20.5%	20.5%
	ϕ= 20%	11.2%	11.2%	11.2%
20-year Term Policy	ϕ= 5%	64.5%	64.5%	64.5%
	ϕ= 10%	33.8%	33.8%	33.8%
	ϕ= 20%	18.4%	18.4%	18.4%

pricing effect of ignoring aggregate lapsation risk. If the artificially higher discounting curve offsets some of the mispricing effect, then life insurers may have been accidentally pricing life insurance policies closer to the theoretically correct price than what we calculate in Section 5.6. Table 8 shows the results from applying higher discount curves than the Treasury curve.[17] By ignoring aggregate lapsation risk, life insurers effectively use lapsation rates that are too low when pricing their policies, compared to the risk-neutral lapsation rates. This leads them to overstate their expected premium income and their expected death benefit payouts. Using a higher discount rate in these present value calculations effectively offsets the effect of using lapsation rates that are too high. As a result, the "double mispricing" effects in Table 8 are much smaller than in Table 7. Life insurers may get the pricing about right, but it is only because two mistakes cancel each other out.

6 Conclusion

We study aggregate lapsation risk in the life insurance sector. Using regulatory filings, we document the counter-cyclicality of lapsation behavior. Two lapsation risk factors explain a large part of the common variation in the lapsation rates of the 30 largest life insurance companies. The first is a cyclical factor that correlates with the credit spread and employment, while the second factor is a trend factor that correlations with the level of interest rates. Using a novel policy-level database from a large life insurer, we examine the heterogeneity in risk factor exposures based on policy and policyholder characteristics. Young policyholders with higher health risks display more cyclical lapsation behavior. We explore the implications for hedging and valuation of life insurance contracts. Ignoring aggregate lapsation risk results in cross-subsidization across policyholders with different lapsation risk, and in mispriced insurer premiums and profits. Our results have implications for the welfare costs of business cycles.

[17] The Standard Valuation Model published by NAIC contains a reserve calculation with a discount rate based on a moving average of the Moody's average composite yields of seasoned corporate bonds. The actual discount rate formula used is $I = 0.03 + \rho \cdot (\min(R, 0.09) - 0.03) + (\rho/2) * (\max(R, 0.09) - 0.09)$, where R is the minimum of the 12-months and the 36-months moving average of the Moody's composite yield on seasoned corporate bonds. To mimic this formula, we assume that the insurer uses the risk-free discounting curve implied by the alternative log SDF, $m^*_{t+1} = -0.03 - \rho(y^{\$}_{t,1} + s_t - 0.03) - \frac{1}{2}\Lambda'_t\Lambda_t - \Lambda'_t\varepsilon_{t+1}$. We use the parameter $\rho = 0.45$, as specified in Section 2.a.iii of VM-20 (National Association of Insurance Commissioners, 2021) for policies with duration between 10 and 20 years. The implied credit spread over Treasury curve is around 1.2% to 1.5% across different maturities. Effectively, we are shifting up the discount rate by 1.2-1.5% points relative to the Treasury yield curve.

Table 8. **Double Mispricing with Credit Discounting**

This table presents the calculated mispricing measure defined in Section 5.6 by

$$Mispricing(\%) = \frac{V^{realized} - V^{correct}}{V^{correct}}$$

where $V^{correct} = \hat{\phi}\beta(T)$ is the correct profit of selling the term policy at markup $\hat{\phi}$ assuming the correct pricing. $V^{realized} = \tilde{p} \cdot (\alpha(T) - \kappa) - \beta(T)$ is the realized valuation based on the assumption that the premium $\tilde{p}$ is doubly-mispriced, i.e. the aggregate lapsation risk is ignored but also the credit curve is used for discounting. See 5.7 for the details.

Mispricing (%)				
		κ=0.5	κ=0.75	κ=1.0
10-year Term Policy	ϕ= 5%	-11.5%	-10.3%	-9.0%
	ϕ= 10%	-6.0%	-5.4%	-4.7%
	ϕ= 20%	-3.3%	-2.9%	-2.6%
15-year Term Policy	ϕ= 5%	1.4%	1.9%	2.6%
	ϕ= 10%	0.7%	1.0%	1.3%
	ϕ= 20%	0.4%	0.6%	0.7%
20-year Term Policy	ϕ= 5%	18.4%	18.6%	18.8%
	ϕ= 10%	9.6%	9.7%	9.9%
	ϕ= 20%	5.3%	5.3%	5.4%
Fixed-Cost Effect (%)				
		κ=0.5	κ=0.75	κ=1.0
10-year Term Policy	ϕ= 5%	2.1%	3.2%	4.5%
	ϕ= 10%	1.1%	1.7%	2.4%
	ϕ= 20%	0.6%	0.9%	1.3%
15-year Term Policy	ϕ= 5%	1.1%	1.6%	2.3%
	ϕ= 10%	0.6%	0.9%	1.2%
	ϕ= 20%	0.3%	0.5%	0.7%
20-year Term Policy	ϕ= 5%	0.4%	0.5%	0.7%
	ϕ= 10%	0.2%	0.3%	0.4%
	ϕ= 20%	0.1%	0.2%	0.2%
Mortality Effect (%)				
		κ=0.5	κ=0.75	κ=1.0
10-year Term Policy	ϕ= 5%	-13.5%	-13.5%	-13.5%
	ϕ= 10%	-7.1%	-7.1%	-7.1%
	ϕ= 20%	-3.9%	-3.9%	-3.9%
15-year Term Policy	ϕ= 5%	0.3%	0.3%	0.3%
	ϕ= 10%	0.2%	0.2%	0.2%
	ϕ= 20%	0.1%	0.1%	0.1%
20-year Term Policy	ϕ= 5%	18.1%	18.1%	18.1%
	ϕ= 10%	9.5%	9.5%	9.5%
	ϕ= 20%	5.2%	5.2%	5.2%

References

Boyarchenko, Nina, Andreas Fuster, and David O. Lucca. 2019. "Understanding Mortgage Spreads." *Review of Financial Studies* 32 (10):3799–3850.

Chernov, Mikhail, Brett R. Dunn, and Francis A. Longstaff. 2018. "Macroeconomic-Driven Prepayment Risk and the Valuation of Mortgage-Backed Securities." *Review of Financial Studies* 31 (3):1132–1183.

Deng, Yongheng, John M. Quigley, and Robert Van Order. 2000. "Mortgage Terminations, Heterogeneity and the Exercise of Mortgage Options." *Econometrica* 68 (2):275–307.

Diep, Peter, Andrea L. Eisfeldt, and Scott Richardson. 2021. "The Cross Section of MBS Returns." *Journal of Finance* 76 (5):2093–2151.

Eling, Martin and Dieter Kiesenbauer. 2013. "What Policy Features Determine Life Insurance Lapse? An Analysis of the German Market." *Journal of Risk and Insurance* 81 (2):241–269.

Fisher, Jack, Alessandro Gavazza, Lu Liu, Tarun Ramadorai, and Jagdish Tripathy. 2021. "Refinancing Cross-Subsidies in the Mortgage Market." Working Paper.

Gerardi, Kristopher, Paul Willen, and David Hao Zhang. 2021. "Mortgage Prepayment, Race, and Monetary Policy." Working Paper.

Gottlieb, Daniel and Kent Smetters. 2021. "Lapse-Based Insurance." *American Economic Review* 111 (8):2377–2416.

Hamilton, James D. 2018. "Why You Should Never Use the Hodrick-Prescott Filter." *The Review of Economics and Statistics* 100 (5):831–843.

Hendel, Igal and Alessandro Lizzeri. 2003. "The Role of Commitment in Dynamic Contracts: Evidence from Life Insurance." *Quarterly Journal of Economics* 118 (1):299–328.

Kuo, Weiyu, Chenghsien Tsai, and Wei-Kuang Chen. 2003. "An Empirical Study on the Lapse Rate: The Cointegration Approach." *Journal of Risk and Insurance* 70 (3):489–508.

Milliman. 2020. "MIMSA III 2020: Study on Mortality and Lapse Rates in Level Term Life Insurance." Milliman Research Report.

National Association of Insurance Commissioners. 2021. "Valuation Manual: Jan 1, 2022 Edition."

Schwartz, Eduardo S. and Walter N. Torous. 1989. "Prepayment and the Valuation of Mortgage-Backed Securities." *Journal of Finance* 44 (2):375–392.

Society of Actuaries. 2010. "Report on the Lapse and Mortality Experience of Post-Level Premium Period Term Plans."

Society of Actuaries and LIMRA. 2012. "U.S. Individual Life Insurance Persistency: A Joint Study Sponsored by the Society of Actuaries and LIMRA."

———. 2019. "U.S. Individual Life Insurance Persistency: A Joint Study Sponsored by the Society of Actuaries and LIMRA."

Stanton, Richard. 1995. "Rational Prepayment and the Valuation of Mortgage-Backed Securities." *Review of Financial Studies* 8 (3):677–708.

Zhang, David. 2022. "Closing Costs, Refinancing, and Inefficiencies in the Mortgage Market." Working Paper.

A Model Solution

A.1 Nominal Bonds

Proposition 1. Nominal bond yields are affine in the state vector:

$$y_t^{\$}(\tau) = -\frac{A_\tau^{\$}}{\tau} - \frac{B_\tau^{\$\prime}}{\tau} z_t,$$

where the coefficients $A_\tau^{\$}$ and $B_\tau^{\$}$ satisfy the following recursions:

$$A_{\tau+1}^{\$} = A_\tau^{\$} + \frac{1}{2}\left(B_\tau^{\$}\right)' \Sigma \left(B_\tau^{\$}\right) + \left(B_\tau^{\$}\right)' \left(\mu - \Sigma^{\frac{1}{2}} \Lambda_0\right), \tag{A.1}$$

$$\left(B_{\tau+1}^{\$}\right)' = \left(B_\tau^{\$}\right)' \left(\Psi - \Sigma^{\frac{1}{2}} \Lambda_1\right) - e_{yn}', \tag{A.2}$$

initialized at $A_0^{\$} = 0$ and $B_0^{\$} = 0$.

Proof. We conjecture that the $t+1$-price of a τ-period bond is exponentially affine in the state:

$$\log(P_{t+1,\tau}^{\$}) = A_\tau^{\$} + \left(B_\tau^{\$}\right)' z_{t+1}$$

and solve for the coefficients $A_{\tau+1}^{\$}$ and $B_{\tau+1}^{\$}$ in the process of verifying this conjecture using the Euler equation:

$$\begin{aligned} P_{t,\tau+1}^{\$} &= \mathbb{E}_t[\exp\{m_{t+1}^{\$} + \log\left(P_{t+1,\tau}^{\$}\right)\}] \\ &= \mathbb{E}_t[\exp\{-y_{t,1}^{\$} - \frac{1}{2}\Lambda_t'\Lambda_t - \Lambda_t'\varepsilon_{t+1} + A_\tau^{\$} + \left(B_\tau^{\$}\right)' z_{t+1}\}] \\ &= \exp\{-e_{yn}' z_t - \frac{1}{2}\Lambda_t'\Lambda_t + A_\tau^{\$} + \left(B_\tau^{\$}\right)'(\mu + \Psi z_t)\} \times \\ &\quad \mathbb{E}_t\left[\exp\{-\Lambda_t'\varepsilon_{t+1} + \left(B_\tau^{\$}\right)' \Sigma^{\frac{1}{2}} \varepsilon_{t+1}\}\right]. \end{aligned}$$

We use the log-normality of ε_{t+1} and substitute for the affine expression for Λ_t to get:

$$P_{t,\tau+1}^{\$} = \exp\left\{-e_{yn}' z_t + A_\tau^{\$} + \left(B_\tau^{\$}\right)'(\mu + \Psi z_t) + \frac{1}{2}\left(B_\tau^{\$}\right)' \Sigma \left(B_\tau^{\$}\right) - \left(B_\tau^{\$}\right)' \Sigma^{\frac{1}{2}} (\Lambda_0 + \Lambda_1 z_t)\right\}.$$

Taking logs and collecting terms, we obtain a linear equation for $\log(p_t(\tau+1))$:

$$\log\left(P_{t,\tau+1}^{\$}\right) = A_{\tau+1}^{\$} + \left(B_{\tau+1}^{\$}\right)' z_t,$$

where $A_{\tau+1}^{\$}$ satisfies (A.1) and $B_{\tau+1}^{\$}$ satisfies (A.2). The relationship between log bond prices

and bond yields is given by $-\log\left(P^{\$}_{t,\tau}\right)/\tau = y^{\$}_{t,\tau}$. □

A.2 Term Life Policy

Proposition 2. Term policy price p can be written as:

$$p = (1+\phi)\frac{\sum_{\tau=1}^{T}\exp\left(P_\tau(b^{(1:\tau-1)},0)+Q_\tau(b^{(1:\tau-1)},0)'z_t\right)\pi_{a+\tau-1}\prod_{s=1}^{\tau-1}(1-\pi_{a+s-1})}{1+\sum_{\tau=1}^{T-1}\exp\left(P_\tau(b^{(1:\tau)})+Q_\tau(b^{(1:\tau)})'z_t\right)\prod_{s=1}^{\tau}(1-\pi_{a+s-1})-\kappa},$$

where the coefficient functions $P_\tau : \mathbb{R}^\tau \to \mathbb{R}$ and $Q_\tau : \mathbb{R}^\tau \to \mathbb{R}^N$ satisfy the following recursions:

$$\begin{aligned} P_{\tau+1}(b^{(1:\tau+1)}) &= -b^{(1)}a_0 + P_\tau(b^{(2:\tau+1)}) + \left(Q_\tau(b^{(2:\tau+1)}) - b^{(1)}a_1\right)'\left(\mu - \Sigma^{\frac{1}{2}}\Lambda_0\right) \\ &\quad + \frac{1}{2}\left(Q_\tau(b^{(2:\tau+1)}) - b^{(1)}a_1\right)'\Sigma\left(Q_\tau(b^{(2:\tau+1)}) - b^{(1)}a_1\right) \qquad \text{(A.3)} \\ \left(Q_{\tau+1}(b^{(1:\tau+1)})\right)' &= \left(Q_\tau(b^{(2:\tau+1)}) - b^{(1)}a_1\right)'\left(\Psi - \Sigma^{\frac{1}{2}}\Lambda_1\right) - e'_{yn}, \qquad \text{(A.4)} \end{aligned}$$

initialized at $P_0 = 0$ and $Q_0 = 0$.

Proof. We conjecture the exponential affine form solution,

$$E_t\left[M^{\$}_{t,1:\tau}\prod_{s=1}^{\tau}(1-\lambda^{(s)}_{t+s})\right] = \exp\left(P_\tau(b^{(1:\tau)}) + Q_\tau(b^{(1:\tau)})'z_t\right)$$

Then we can recursively calculate $E_t\left[M^{\$}_{t,1:\tau+1}\prod_{s=1}^{\tau+1}(1-\lambda^{(s)}_{t+s})\right]$ as the following (we use a concise notation $\vec{b} = b^{(2:\tau+1)}$)

$$
\begin{aligned}
&E_t\left[\prod_{s=1}^{\tau+1}\exp(m^{\$}_{t+s}-b^{(s)}\tilde{l}_{t+s})\right]\\
&=E_t\left[\exp(m^{\$}_{t+1}-b^{(1)}\tilde{l}_{t+1})E_{t+1}\left[\prod_{s=1}^{\tau}\exp(m^{\$}_{t+1+s}-b^{(s+1)}\tilde{l}_{t+1+s})\right]\right]\\
&=E_t\left[\exp(m^{\$}_{t+1}-b^{(1)}\tilde{l}_{t+1})\exp\left[P_\tau(b^{(2:\tau+1)})+Q_\tau(b^{(2:\tau+1)})'z_{t+1}\right]\right]\\
&=E_t\exp\left[(-e'_{yn}z_t-\frac{1}{2}\Lambda_t'\Lambda_t-\Lambda_t'\epsilon_{t+1}-b^{(1)}(a_0+a_1'z_{t+1})+P_\tau(\vec{b})+Q_\tau(\vec{b})'z_{t+1})\right]\\
&=E_t\exp\left[(-e'_{yn}z_t-\frac{1}{2}\Lambda_t'\Lambda_t-\Lambda_t'\epsilon_{t+1}-b^{(1)}a_0+P_\tau(\vec{b}))+(Q_\tau(\vec{b})-b^{(1)}a_1)'z_{t+1})\right]\\
&=E_t\exp\Bigg[(-e'_{yn}z_t-\frac{1}{2}\Lambda_t'\Lambda_t-\Lambda_t'\epsilon_{t+1}-b^{(1)}a_0+P_\tau(\vec{b}))\\
&\qquad+(Q_\tau(\vec{b})-b^{(1)}a_1)'(\mu+\Psi z_t+\Sigma^{\frac{1}{2}}\varepsilon_{t+1}))\Bigg]\\
&=E_t\exp\Bigg[(-\frac{1}{2}\Lambda_t'\Lambda_t-b^{(1)}a_0+P_\tau(\vec{b}))+(Q_\tau(\vec{b})-b^{(1)}a_1)'\mu\\
&\qquad+((Q_\tau(\vec{b})-b^{(1)}a_1)'\Psi-e'_{yn})z_t+((Q_\tau(\vec{b})-b^{(1)}a_1)'\Sigma^{\frac{1}{2}}-\Lambda_t')\varepsilon_{t+1}\Bigg]\\
&=\exp\Bigg[-b^{(1)}a_0+P_\tau(\vec{b})+(Q_\tau(\vec{b})-b^{(1)}a_1)'\mu+((Q_\tau(\vec{b})-b^{(1)}a_1)'\Psi-e'_{yn})z_t\\
&\qquad+\frac{1}{2}(Q_\tau(\vec{b})-b^{(1)}a_1)'\Sigma(Q_\tau(\vec{b})-b^{(1)}a_1)-(Q_\tau(\vec{b})-b^{(1)}a_1)'\Sigma^{\frac{1}{2}}(\Lambda_0+\Lambda_1 z_t)\Bigg]\\
&=\exp\Bigg[-b^{(1)}a_0+P_\tau(\vec{b})+(Q_\tau(\vec{b})-b^{(1)}a_1)'(\mu-\Sigma^{\frac{1}{2}}\Lambda_0)\\
&\qquad+\frac{1}{2}(Q_\tau(\vec{b})-b^{(1)}a_1)'\Sigma(Q_\tau(\vec{b})-b^{(1)}a_1)\\
&\qquad+((Q_\tau(\vec{b})-b^{(1)}a_1)'(\Psi-\Sigma^{\frac{1}{2}}\Lambda_1)-e'_{yn})z_t\Bigg]
\end{aligned}
$$

Taking the logs and collecting terms, we obtain a linear equation:

$$
\log\left(E_t\left[M^{\$}_{t,1:\tau+1}\prod_{s=1}^{\tau+1}(1-\lambda^{(s)}_{t+s})\right]\right)=P_{\tau+1}(b^{(1:\tau+1)})+Q_{\tau+1}(b^{(1:\tau+1)})'z_t
$$

where the coefficient functions satisfy

$$P_{\tau+1}(b^{(1:\tau+1)}) = -b^{(1)}a_0 + P_\tau(b^{(2:\tau+1)}) + (Q_\tau(b^{(2:\tau+1)}) - b^{(1)}a_1)'(\mu - \Sigma^{\frac{1}{2}}\Lambda_0) + \frac{1}{2}(Q_\tau(b^{(2:k+1)}) - b^{(1)}a_1)'\Sigma(Q_\tau(b^{(2:\tau+1)}) - b^{(1)}a_1)$$

and

$$Q_{\tau+1}(b^{(1:\tau+1)})' = (Q_\tau(b^{(2:\tau+1)}) - b^{(1)}a_1)'(\Psi - \Sigma^{\frac{1}{2}}\Lambda_1) - e'_{yn}$$

Substituting $E_t\left[M^{\$}_{t,1:\tau}\prod_{s=1}^{\tau}(1-\lambda^{(s)}_{t+s})\right] = \exp\left(P_\tau(b^{(1:\tau)}) + Q_\tau(b^{(1:\tau)})z_t\right)$ into Equation (8) concludes the proof.

Note that if we evaluate the coefficients with $b^{(n)} = 0, \forall n$, then $\{P_\tau, Q_\tau\}$ do not depend on b anymore, so we get the following recursion for the affine coefficient constants $\{ZP_\tau, ZQ_\tau\}$ for the zero coupon bonds Z_τ (i.e. $Z_\tau = E_t\left[M^{\$}_{t,t+1:t+\tau}\right] = \exp\left[ZP_\tau + ZQ_\tau{}'z_t\right]$)

$$ZP_{\tau+1} = ZP_\tau + ZQ_\tau{}'(\mu - \Sigma^{\frac{1}{2}}\Lambda_0) + \frac{1}{2}ZQ_\tau{}'\Sigma ZQ_\tau$$
$$ZQ_{\tau+1}{}' = ZQ_\tau{}'(\Psi - \Sigma^{\frac{1}{2}}\Lambda_1) - e'_{yn}$$

We can analogously calculate the coefficient function recursion for the expected survival function, $L_\tau(b^{(1:\tau)}) = E_t\left[\prod_{s=1}^{\tau}(1-\lambda^{(s)}_{t+s})\right] = \exp\left[LP_\tau(b^{(1:\tau)}) + LQ_\tau(b^{(1:\tau)})'z_t\right]$

$$LP_{\tau+1}(b^{(1:\tau+1)}) = -b^{(1)}a_0 + LP_\tau(b^{(2:\tau+1)}) + (LQ_\tau(b^{(2:\tau+1)}) - b^{(1)}a_1)'\mu + \frac{1}{2}(LQ_\tau(b^{(2:\tau+1)}) - b^{(1)}a_1)'\Sigma(LQ_\tau(b^{(2:\tau+1)}) - b^{(1)}a_1)$$
$$LQ_{\tau+1}(b^{(1:\tau+1)})' = (LQ_\tau(b^{(2:\tau+1)}) - b^{(1)}a_1)'\Psi$$

□

B Monthly VAR Model Calibration with Annual Data

B.1 Model Setup

We follow the set up described in Section 5.5. The monthly state variables $z_t = (r_t, cr_t, s_t)'$ follows the dynamics

$$z_t = \mu + \Psi z_{t-1} + \Sigma^{\frac{1}{2}}\varepsilon_t \tag{B.1}$$

The monthly dynamics implies the following two annual dynamics

$$z_{t+k} = \left(\sum_{i=0}^{k-1} \Psi^i\right) \mu + \Psi^k z_t + \sum_{i=0}^{k-1} \Psi^i \Sigma^{\frac{1}{2}} \varepsilon_{t+k-i}, \tag{B.2}$$

and

$$\sum_{k=1}^{K} z_{t+k} = \sum_{k=1}^{K} \left(\sum_{i=0}^{k-1} \Psi^i\right) \mu + \sum_{k=1}^{K} \Psi^k z_t + \sum_{k=1}^{K} \sum_{i=0}^{k-1} \Psi^i \Sigma^{\frac{1}{2}} \varepsilon_{t+k-i}. \tag{B.3}$$

Equation (B.2) describes the dynamics of the annually observed interest rate and the credit spread (r_{t+12} and s_{t+12}), while Equation (B.3) describes the annually observed credit return ($\sum_{k=1}^{12} cr_{t+k}$).

The monthly nominal SDF $M^{\$}_{t+1} = \exp(m^{\$}_{t+1})$ becomes

$$m^{\$}_{t+1} = -\frac{\delta_0}{12} - \frac{\delta_1' z_t}{12} - \frac{1}{2}\Lambda_t'\Lambda_t - \Lambda_t' \varepsilon_{t+1}. \tag{B.4}$$

where the one-month discount rate $y^{\$}_{t,1} = \frac{\delta_0}{12} + \frac{\delta_1' z_t}{12}$ is an affine form of the state variable z_t. We parametrize the market price of risk Λ_t as

$$\Lambda_t = \Lambda_0 + \Lambda_1 z_t = \Lambda_0 + \hat{\Lambda}_1 e_3' z_t$$

which requires us to identify three parameters, two for $\Lambda_0 = (\Lambda_0^r, \Lambda_0^{cr}, 0)'$ and one for $\hat{\Lambda}_1 = (0, \zeta, 0)'$.

We additionally model the credit return as

$$cr_{t+1} - y^{\$}_{t,1} = \gamma_0 + \gamma_1 s_t + \sigma^{cr} e_{t+1} \tag{B.5}$$

with $e_{t+1} \sim \mathcal{N}(0,1)$, so that the expected excess return depends on the credit spread.

Note that the recursions in Proposition 1 and Proposition 2 in Appendix A are slightly changed in the monthly model, as the discount rate is now an affine form of the states, not simply the first state. More precisely, Equation (A.1) and (A.2) become

$$A^{\$}_{\tau+1} = -\frac{\delta_0}{12} + A^{\$}_{\tau} + \frac{1}{2}\left(B^{\$}_{\tau}\right)' \Sigma \left(B^{\$}_{\tau}\right) + \left(B^{\$}_{\tau}\right)' \left(\mu - \Sigma^{\frac{1}{2}}\Lambda_0\right), \tag{B.6}$$

$$\left(B^{\$}_{\tau+1}\right)' = \left(B^{\$}_{\tau}\right)' \left(\Psi - \Sigma^{\frac{1}{2}}\Lambda_1\right) - \frac{\delta_1'}{12} \tag{B.7}$$

and Equation (A.3) and (A.4) become

$$\begin{aligned} P_{\tau+1}(b^{(1:\tau+1)}) &= -\frac{\delta_0}{12} - b^{(1)}a_0 + P_\tau(b^{(2:\tau+1)}) + \left(Q_\tau(b^{(2:\tau+1)}) - b^{(1)}a_1\right)' \left(\mu - \Sigma^{\frac{1}{2}}\Lambda_0\right) \\ &\quad + \frac{1}{2}\left(Q_\tau(b^{(2:\tau+1)}) - b^{(1)}a_1\right)' \Sigma \left(Q_\tau(b^{(2:\tau+1)}) - b^{(1)}a_1\right) \qquad \text{(B.8)} \\ \left(Q_{\tau+1}(b^{(1:\tau+1)})\right)' &= \left(Q_\tau(b^{(2:\tau+1)}) - b^{(1)}a_1\right)' \left(\Psi - \Sigma^{\frac{1}{2}}\Lambda_1\right) - \frac{\delta_1'}{12}. \qquad \text{(B.9)} \end{aligned}$$

B.2 Calibration Process

Note that given our specification of Λ_0 and Λ_1, all the affine coefficients for the yields $\{B_\tau^\$\}_{\forall\tau}$ have the second and the third components zeros (see Equation B.7), so we can simplify to $\delta_1 = (\hat{\delta}_1, 0, 0)$ and only need to estimate $\hat{\delta}_1$. Then the short rate then becomes $12y_{t,1}^\$ = \delta_0 + \delta_1' z_t = \delta_0 + \hat{\delta}_1 r_t$.

We start by restricting the companion matrix as

$$\Psi = \begin{bmatrix} \phi_r & 0 & 0 \\ \frac{\hat{\delta}_1}{12} & 0 & \gamma_1 \\ 0 & 0 & \phi_s \end{bmatrix}$$

The restriction in the second row directly follows from our credit return model in Equation (B.5). For r_t and s_t, we set the off-diagonal terms zero. For the covariance matrix, we specify is as a lower triangular matrix

$$\Sigma^{\frac{1}{2}} = \begin{bmatrix} \sigma^{11} & 0 & 0 \\ \sigma^{21} & \sigma^{22} & 0 \\ \sigma^{31} & \sigma^{32} & \sigma^{33} \end{bmatrix}$$

The monthly persistence parameters (ϕ_r, ϕ_s) are estimated by regressing r_{t+12} on r_t and s_{t+12} on s_t, as Equation (B.2) implies

$$r_{t+12} = e_1' \left(\sum_{i=0}^{k-1} \Psi^i\right) \mu + e_1' \Psi^k z_t + e_1' \sum_{i=0}^{11} \Psi^i \Sigma^{\frac{1}{2}} \varepsilon_{t+12-i} \qquad \text{(B.10)}$$

$$s_{t+12} = e_3' \left(\sum_{i=0}^{k-1} \Psi^i\right) \mu + e_3' \Psi^k z_t + e_3' \sum_{i=0}^{11} \Psi^i \Sigma^{\frac{1}{2}} \varepsilon_{t+12-i}. \qquad \text{(B.11)}$$

That is, Ψ^{12} is the annual companion matrix. The estimated annual persistence implies $\phi_r^{12} = 0.7770$ and $\phi_s^{12} = 0.2431$, so we get $\phi_r = 0.9792$ and $\phi_s = 0.8888$. We estimate $\mu^r = 0.0006$ and $\mu^s = 0.0026$ to match the unconditional r_t, s_t implied by Equation (B.2) with the 1990-2020

mean in the data, 0.0276 and 0.0237.

Equation (B.10) also implies that the error term of r_{t+12} on r_t regression is $e_1' \sum_{i=0}^{11} \Psi^i \Sigma^{\frac{1}{2}} \varepsilon_{t+12-i}$. Then the variance of the error term becomes

$$Var_t[e_1' \sum_{i=0}^{11} \Psi^i \Sigma^{\frac{1}{2}} \varepsilon_{t+12-i}] = \sum_{i=0}^{11} e_1' \Psi^i \Sigma (\Psi^i)' e_1 \tag{B.12}$$

which implies $\sigma^{11} = 0.0041$.

We then estimate $(\Lambda_0^r, \delta_0, \hat{\delta}_1)$ using the following three moment conditions. First, we match the unconditional slope of the yield curve between the 1-year and 10-year log rates, which is 0.136 in the 1990-2020 annual data. We also match $A_{12}^{\$} = 0$ and $B_{12}^{\$} = (-1, 0, 0)$ conditions. Note that given our risk price assumption, knowing μ^r and σ^{11} is sufficient to generate the entire yield curve. The estimated parameters are $\Lambda_0^r = -0.1265$, $\delta_0 = -0.0062$ and $\hat{\delta}_1 = 1.1196$.

Now we estimate γ_1. First, observe that the dynamics of $\sum_{k=1}^{12} cr_{t+k}$ is implied by Equation (B.3)

$$\sum_{k=1}^{12} cr_{t+k} = e_2' \sum_{k=1}^{12} \left(\sum_{i=0}^{k-1} \Psi^i \right) \mu + e_2' \sum_{k=1}^{12} \Psi^k z_t + e_2' \sum_{k=1}^{12} \sum_{i=0}^{k-1} \Psi^i \Sigma^{\frac{1}{2}} \varepsilon_{t+k-i} \tag{B.13}$$

Observe that $e_2' \sum_{k=1}^{12} \Psi^k = (1, 0, \left(\sum_{i=0}^{11} \phi_s^i \right) \gamma_1)$. Therefore if we regress $\left(\sum_{k=1}^{12} cr_{t+k} \right) - r_t$ on s_t, i.e. if we run the annual credit excess return predictive regression, the estimated annual prediction coefficient 4.9324 implies $\gamma_1 = 0.7245$. By matching the unconditional credit excess return, we get $\mu^{cr} = -0.0139$.

The rest five elements of $\Sigma^{\frac{1}{2}}$ can be estimated from Equation (B.10), (B.11), and (B.13), which imply 5 covariance equations in addition to Equation (B.12) we already used. For example, the model implied covariance between the residuals of r_{t+12} equation and $\sum_{k=1}^{12} cr_{t+k}$ equation is:

$$Cov_t[e_1' \sum_{i=0}^{11} \Psi^i \Sigma^{\frac{1}{2}} \varepsilon_{t+12-i}, e_2' \sum_{k=1}^{12} \sum_{i=0}^{k-1} \Psi^i \Sigma^{\frac{1}{2}} \varepsilon_{t+k-i}]$$

which should match the (1, 2)-th element of the residual covariance matrix from the regressions in Equation (B.10), (B.11), and (B.13) using the annual data. The estimated $\Sigma^{\frac{1}{2}}$ is:

$$\Sigma^{\frac{1}{2}} = \begin{bmatrix} 0.0041 & 0 & 0 \\ 0.0013 & 0.0242 & 0 \\ -0.0023 & -0.0025 & 0.0016 \end{bmatrix}$$

We conclude the calibration process by estimating the rest two market price of risks, Λ_0^{cr} and ζ. We use the conditions from the credit return Euler equations, Equation (15) and (16) that we specify in Section 5.5 as moment conditions:

$$\gamma_0 + \gamma_1 E[s_t] + \frac{1}{2}(\sigma^{cr})^2 = \Lambda_0^r \sigma^{cr} Cov[e_{t+1}, \varepsilon_{t+1}^r] + (\Lambda_0^{cr} + \zeta E[s_t])\sigma^{cr} Cov[e_{t+1}, \varepsilon_{t+1}^{cr}] \tag{B.14}$$

$$\gamma_1 = \zeta \sigma^{cr} Cov[e_{t+1}, \varepsilon_{t+1}^{cr}] \tag{B.15}$$

where $(\sigma^{cr})^2 = \Sigma_{2,2}$, $\sigma^{cr} Cov[e_{t+1}, \varepsilon_{t+1}^r] = \Sigma_{2,1}^{\frac{1}{2}}$, and $\sigma^{cr} Cov[e_{t+1}, \varepsilon_{t+1}^{cr}] = \Sigma_{2,2}^{\frac{1}{2}}$. The estimated parameters are $\Lambda_0^{cr} = -0.5365$ and $\zeta = 29.98$.

B.3 Mispricing Calculation with Monthly VAR Model

Proposition 2 assumes the annual VAR model. Pricing formula and mispricing calculation should be slightly modified to reflect the fact that (i) we model the underlying monthly VAR model, and (ii) we model the lapse factor as a function of the 12-month moving average of the states, i.e. $\tilde{l}_t = a_0 + a_1' \bar{z}_t$. Equation (B.6), (B.7), (B.8), and (B.9) show how the recursions change due to the monthly SDF specification (effect of (i)). We additionally modify the recursions Equation (B.8) and (B.9) in this section (effect of (ii)).

We extend the state space to include the 11 lagged state variables, i.e. $y_t' = (z_t', z_{t-1}', \cdots, z_{t-11}')$. Then the dynamics of y_t is derived from Equation (B.1):

$$y_t = \tilde{\mu} + \tilde{\Psi} y_{t-1} + \tilde{\Sigma}^{\frac{1}{2}} \varepsilon_t$$

where the new parameters $(\tilde{\mu}, \tilde{\Psi}, \tilde{\Sigma}^{\frac{1}{2}})$ can be naturally extended from $(\mu, \Psi, \Sigma^{\frac{1}{2}})$ by padding zeros and identity matrices. We can similarly extend the time-varying component of MPR Λ_1 to $\tilde{\Lambda}_1$. We omit the details for brevity.

We can also transform the parameters $a_0, a_1, \{b^{(n)}\}$ to be consistent with the extended state space. The lapse factor can be written as $\tilde{l}_t = a_0 + a_1' \bar{z}_t = a_0 + \tilde{a}_1' y_t$, where $\tilde{a}_1' = (\frac{1}{12}, \frac{1}{12}, \ldots, \frac{1}{12}) \otimes a_1'$. Also define $\{\tilde{b}^{(n)}\}_{1 \le n \le 240}$ as

$$\tilde{b}^{(n)} = \begin{cases} 0 & if \quad \text{mod } (n, 12) \neq 0 \\ b^{(n/12)} & if \quad \text{mod } (n, 12) = 0 \end{cases}$$

Then we can calculate the monthly recursions similar to Proposition 2,

$$\begin{aligned} P_{\tau+1}(\tilde{b}^{(1:\tau+1)}) &= -\frac{\delta_0}{12} - \tilde{b}^{(1)}a_0 + P_\tau(\tilde{b}^{(2:\tau+1)}) + \left(Q_\tau(\tilde{b}^{(2:\tau+1)}) - \tilde{b}^{(1)}\tilde{a}_1\right)' \left(\tilde{\mu} - \tilde{\Sigma}^{\frac{1}{2}}\Lambda_0\right) \\ &\quad + \frac{1}{2}\left(Q_\tau(\tilde{b}^{(2:\tau+1)}) - \tilde{b}^{(1)}\tilde{a}_1\right)' \tilde{\Sigma} \left(Q_\tau(\tilde{b}^{(2:\tau+1)}) - \tilde{b}^{(1)}\tilde{a}_1\right) \qquad \text{(B.16)} \\ \left(Q_{\tau+1}(\tilde{b}^{(1:\tau+1)})\right)' &= \left(Q_\tau(\tilde{b}^{(2:\tau+1)}) - \tilde{b}^{(1)}\tilde{a}_1\right)' \left(\tilde{\Psi} - \tilde{\Sigma}^{\frac{1}{2}}\tilde{\Lambda}_1\right) - \frac{\delta_1'}{12}. \qquad \text{(B.17)} \end{aligned}$$

Note that after calculating the monthly coefficient recursions, we still calculate the premium leg and the death benefit leg value by summing up annual strips, where the τth-year strip is calculated by:

$$E_t\left[M^{\$}_{t,1:\tau}\prod_{s=1}^{\tau}(1-\lambda^{(s)}_{t+s})\right] = \exp\left(P_{12*\tau}(\tilde{b}^{(1:12*\tau)}) + Q_{12*\tau}(\tilde{b}^{(1:12*\tau)})'y_t\right).$$

C Markup Validation with Expected Profit Share

The life insurer sets ϕ as the markup on the policy before considering the brokerage fee. From the net premium (the expected premium income net of the expected benefit payout) the insurer first pays the broker fee and the rest is the earned profit. In presenting mispricing results, we vary ϕ to take values of 5%, 10%, and 20%. To validate whether these values are realistic, we calculate the expected profit split of $\theta : (1-\theta)$ between the insurer and the broker, where $0 < \theta < 1$ indicates the life insurer's profit share and the $(1-\theta)$ indicates the broker fee share. The premium pricing formula from Section 5.6 is

$$\begin{aligned}\tilde{p} &= (1+\phi)\frac{E_t\left[\sum_{\tau=1}^{T} M^{\$}_{t,1:\tau}\pi_{a+\tau-1}\prod_{s=1}^{\tau-1}(1-\pi_{a+s-1})\prod_{s=1}^{\tau-1}(1-\lambda^{(s)}_{t+s})\right]}{E_t\left[1+\sum_{\tau=1}^{T-1} M^{\$}_{t,1:\tau}\prod_{s=1}^{\tau}(1-\pi_{a+s-1})\prod_{s=1}^{\tau}(1-\lambda^{(s)}_{t+s})\right]-\kappa},\\ &= (1+\phi)\frac{\tilde{\beta}(T)}{\tilde{\alpha}(T)-\kappa}\end{aligned}$$

The second line follows from our assumption that the life insurer is pricing premium with markup ϕ without the aggregate lapsation risk. Thus, the expectation operator in the denominator is evaluated to be $\tilde{\alpha}(T)$ instead of $\alpha(T)$, using the notation from Section 5.6.

The life insurer expects $\phi\tilde{\beta}(T)$ as its profit, while the broker receives the fee $\kappa \cdot \tilde{p}$. Therefore, the expected profit share of the insurer is

$$\begin{aligned}\theta &= \frac{\phi\tilde{\beta}(T)}{\phi\tilde{\beta}(T)+\kappa\cdot\tilde{p}}\\ &= \frac{\tilde{\alpha}(T)-\kappa}{(1+\phi^{-1})+\tilde{\alpha}(T)-\kappa}\end{aligned}$$

The formula is consistent with our intuition as the expected profit share θ is higher when the markup (ϕ) is higher and the the broker fee (κ) is lower.

Table A1 shows the expected profit share θ calculated for the ranges of parameters for ϕ and κ we consider in Table 7. In our baseline case of $\phi = 10\%$ and $\kappa = 0.75$, the expected profit share is between 40% to 50%, which is within the range of the industry consensus.

Table A1. **Expected Profit Share**

This table presents the expected profit share θ calculated for the ranges of parameters for ϕ and κ we consider in Table 7. See Appendix C for the details.

		κ=0.5	κ=0.75	κ=1.0
10-year Term Policy	ϕ= 5%	36.0%	26.4%	20.5%
	ϕ= 10%	51.8%	40.6%	32.9%
	ϕ= 20%	66.3%	55.7%	47.4%
15-year Term Policy	ϕ= 5%	41.3%	31.1%	24.7%
	ϕ= 10%	57.3%	46.3%	38.5%
	ϕ= 20%	71.1%	61.3%	53.4%
20-year Term Policy	ϕ= 5%	44.1%	33.8%	27.0%
	ϕ= 10%	60.1%	49.3%	41.4%
	ϕ= 20%	73.4%	64.1%	56.5%

D Additional Tables and Figures

Table A2. **Lapse Rate Change against County-level Economic Variables: OLS**

This table reports the county-level regression of the change in lapse rates between 2006 and 2009 on the changes in economic variables between 2006 and 2009. We estimate the following cross-sectional regression:

$$(\Delta Lapse06-09)_c = \beta_0 + \beta_1 * (\Delta HousingPrice06-09)_c + \beta_2 * (\Delta Unemp06-09)_c + \gamma * X_c + \varepsilon_c.$$

Robust standard errors are reported.

	Lapse Chg (1)	Lapse Chg (2)	Lapse Chg (3)	Lapse Chg (4)	Lapse Chg (5)	Lapse Chg (6)	Lapse Chg (7)	Lapse Chg (8)	Lapse Chg (9)
Δ Housing Price 06-09	-0.03956***	-0.03710**	-0.03595**				-0.02534	-0.01619	-0.01441
	(0.01370)	(0.01467)	(0.01476)				(0.01618)	(0.01846)	(0.01879)
Δ Unemp 06-09				0.31207***	0.32883***	0.32494***	0.20614	0.25729*	0.26104*
				(0.10234)	(0.10292)	(0.10290)	(0.12606)	(0.13471)	(0.13568)
ACS Income 2006		0.00009	0.00008		0.00024*	0.00021		0.00020	0.00019
		(0.00014)	(0.00014)		(0.00013)	(0.00013)		(0.00015)	(0.00015)
Log Population 2006			0.00015			0.00033			0.00019
			(0.00044)			(0.00040)			(0.00044)
Constant	0.00590***	0.00174	0.00063	-0.00531	-0.01780**	-0.01969**	-0.00208	-0.01360	-0.01523
	(0.00214)	(0.00741)	(0.00818)	(0.00464)	(0.00873)	(0.00912)	(0.00495)	(0.01059)	(0.01145)
R^2	0.01037	0.01075	0.01096	0.01148	0.01483	0.01589	0.01402	0.01583	0.01616
Adj R^2	0.00906	0.00815	0.00705	0.01028	0.01243	0.01228	0.01141	0.01192	0.01094
N	762	762	762	823	823	823	759	759	759

Standard errors in parentheses

* p<0.1, ** p<0.05, *** p<0.01